ABSTRACT

Title of Thesis: COUPLING MECHANISMS
USING 3D-INTEGRATION
FOR NONLINEAR INTEGRATED PHOTONICS

Tahmid Sami Rahman
Master of Science, 2023

Thesis Directed by: Dr. Kartik Srinivasan
Department of Physics

Improving coupling between integrated photonics chips and optical fibers is an important topic of study for many applications. For photonic integrated circuits, different coupling methods have been implemented including edge coupling, grating coupling and 3D-integration using direct laser writing. Silicon nitride is a widely proven material for non linear optical phenomena such as frequency comb, optical parametric oscillation etc. Here in this thesis, coupling mechanisms based on direct laser writing are presented for use in nonlinear integrated photonics. Simulation works show that a polymer tapered coupler printed on a single mode fiber could be a good alternative to a cleaved fiber and equivalent to a lensed fiber. It is also shown that an out-of-plane polymer coupler on a silicon nitride access waveguide could be a prospective alternative for coupling to nonlinear integrated photonic circuits while avoiding chip separation and facet polishing. Both mechanisms could be good coupling options for shorter wavelength applications.

COUPLING MECHANISMS USING 3D-INTEGRATION FOR NONLINEAR INTEGRATED PHOTONICS

by

Tahmid Sami Rahman

Thesis submitted to the Faculty of the Graduate School of the
University of Maryland, College Park in partial fulfillment
of the requirements for the degree of
Master of Science
2023

Advisory Committee:
Dr. Kartik Srinivasan, Co-Chair/Research Superviser
Dr. Edo Waks, Co-Chair/Advisor
Dr. Yanne Chembo

Acknowledgments

I would like to express my cordial gratitude to a few persons who have encouraged me in technical details as well as moral support that led me to this thesis.

First and foremost I'd like to thank my research supervisor, Dr. Kartik Srinivasan for giving me the opportunity to work on a tool that is unique for 3D integration for optical experiments. Our weekly meetings have always been effective for me to learn things in a better way. I have also been fortunate to utilize a number of opportunities to familiarize myself with a lot of basic understanding. It has been a pleasure to work under his supervision.

I would also like to thank my academic advisor, Dr. Edo Waks. Since I have been a student from Electrical and Computer Engineering, I have always got the opportunity to be enrolled into research credits under his affiliation. He has been very supportive whenever I have faced the need to discuss.

My teammembers in the nanophotonics group have always been helpful towards any technical issue that I have faced. I cannot thank Edgar Perez enough for helping me with the first experience of using nanoscribe tool and a lot more supports. I would like to mention Gregory Moille for setting up the UMD lab for our group that works as a platform for all the UMD students to do experiments. Also I would like to mention other members Khoi, Rahul, Michal, Xiyuan, Roy, Jordan, Ashutosh as well who have always had interaction with me regarding discussion of any research project. I specially would like to mention Daron Westly from NIST who was very

supportive to help me get trained on a lot of day-to-day fabrication tool for our group.

I also acknowledge the Joint Quantum Institute and Electrical and Computer Engineering department to take care of my financial funding scenario as well as Physics purchasing for enabling easy shipping for the experiment orders.

I convey my special thanks to my family-my parents, sister, parents in law and sister in law who have been a moral support during my graduate life from abroad. But a profound gratitude towards my wife, Uzma and my son, Arzad for filling my life with joy and a reason to be motivated.

As friends, brothers and sisters from other mothers, I would like to mention a few senior names Zajeba, Shaolin, Tanvir, Ashis and a lot of junior names including Sayma, Amit, Uday, Pial who have always been supportive to me.

It is impossible to take all the names, and I beg pardon to those I've inadvertently left out.

Thank you all!

Table of Contents

Bibliography 57

List of Tables

List of Figures

List of Abbreviations

AAA	Antiaircraft artillery
ABCCC	Airborne Battlefield Command and Control Center
AEHF	Advanced Extremely High Frequency
AGM	Air-to-ground guided missile
AIT	Assembly, Integration, and Testing
AOR	Area of Responsibility
APAM	Anti-personnel, anti-material
ASOC	Air Support Operations Center
ATACM	Army Tactical Missile System
ATO	Air Tasking Order
AWACS	Airborne Warning and Control System
BAT	Brilliant Ani-Armor Submunition
BDA	Bomb-damage assessment
BFT	Blue Force Tracking
BLOS	Beyond Line-of-Sight
BMD	Ballistic Missile Defense
C^3	Command, Control, and Communications
CAFMS	Computer-aided Force Management System
CALCM	Conventional Air-Launched Cruise Missile
CBU	Cluster Bomb Unit
CCAFS	Cape Canaveral Air Force Station
CENTAF	CENTCOM's Air Force component
CENTCOM	U.S. Central Command
CINC	Commander-in-Chief
CONUS	Continental United States
DAGR	Defense Advanced GPS Reciever
DMA	Defense Mapping Agency
DOD	Department of Defense
DOP	Dilution of Precision
DOT	Department of Transportation
DSMAC	Digital Scene Mapping Area Correlator

EFOG-M	Enhanced Fiber Optic Guided Missile
FAA	Federal Aviation Administration
FLIR	Forward-looking infrared
GAM	Global Positioning System Aided Munition
GPS	Global Positioning System
GWAPS	Gulf War Air Power Survey
HARM	High-Speed Antiradiation Missile
HEO	Highly Elliptical Orbit
IADS	Integrated Air Defense System
ICBM	Inter-Continental Ballistic Missile
INS	Inertial navigation system
IIR	Imaging infrared
IR	Infrared
ISR	Intelligence, Surveillance, and Reconnaissance
JDAM	Joint Direct Attack Munition
JFC	Joint Force Commander
JSOW	Joint Standoff Weapon
LANTIRN	Low-Altitude Navigation and Targeting Infrared for Night System
LEO	Low Earth Orbit
LGB	Laser-guided bomb
MAJIC	Microsatellte Area-Wide Joint Information Communication
MARCENT	CENTCOM's Marine component
MARS	Mid-Atlantic Regional Spaceport
MLRS	Multiple Launch Rocket System
MUOS	Mobile User Objective System
NASA	National Aeronautics and Space Administration
NAVCENT	CENTCOM's Navy component
NPOESS	National Polar-Orbiting Operational Environmental Satellite System
ORS	Opertionally Responsive Space
ORSO	Operationally Responsive Space Office

PDOP	Position Dilution of Precision
PGM	Precision-guided munition
P^3I	Preplanned Product Improvement
PnP	Plug and Play
PnPSat	Plug and Play Satellite
PPS	Precise Positioning Service
RCS	Radar cross section
SA	Situational Awareness
SADARM	Sense and Destroy Armor Munition
SAM	Surface-to-air missile
SAR	Synthetic aperture radar
SBIRS	Space Based Infrared System
SEAD	Suppression of enemy air defenses
SFW	Sensor Fuzed Weapon
SIGINT	Signal Intelligence
SLAM	Standoff Land Attack Missile
SLAM-ER	SLAM-Expanded Response
SpaceX	Space Exploration Technologies Corporation
SPS	Standard Positioning Service
TACC	Tactical Air Control Center
TACS	Tactical Air Control System
TACP	Tactical Air Control Party
TASM	Tomahawk Anti-Ship Missile
TBIP	Tomahawk Baseline Improvement Program
TERCOM	Terrain Contour Mapping
TFR	Terrain-following radar
TLAM	Tomahawk Land Attack Missile
USAF	U.S. Air Force
VAFB	Vandenberg Air Force Base
WGS	Wideband Global SATCOM

Chapter 1: Introduction

1.1 Direct Laser Writing with Two Photon Polymerization

Direct laser writing [2] is a 3D printing technique that uses lasers to selectively solidify or remove materials for creating any complex three-dimensional structures. This 3D-integration process includes a laser beam that is focused to a specific point to polymerize or melt a polymer material, allowing for precise control over the 3D printing process. This technique is often used in microfabrication, photolithography, and the production of microdevices and microstructures. Direct Laser Writing is also known as Two-Photon Polymerization [17] since it uses a nonlinear optical phenomena called two-photon absorption [21]. Two-photon polymerization-based direct laser writing uses ultrashort laser pulses to initiate polymerization in a photosensitive polymer material, where two photons are absorbed simultaneously to start the polymerization reaction. Once the correct objective and polymer resin combination is chosen, this technique allows for high-resolution fabrication of a computer aided design three-dimensional structures at the micro and nanoscale. After 3D-integration, a comparison is needed to verify with reference to the design. This could be done using scanning electron microscopy.

Figure 1.1 shows a photonic GT2 setup for using direct laser writing. The Photonic Professional GT2 is a 3D printer produced by Nanoscribe, a manufacturer based in Germany. It uses the Two-photon polymerization technology to print using negative photoresins. It offers a build volume of

Figure 1.1: This is exactly similar to the Nanoscribe Setup (Image taken from https://www.nanoscribe.com/en/products/photonic-professional-gt2/) that was used for my 3D integration purposes.

Objective					
Mag, WD	10x, 700um	20x	25x, 380um	63x, 190um	63x
	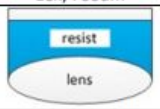	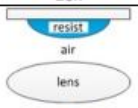	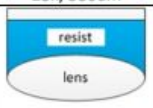		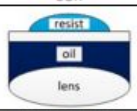
Application area	um to mm 3D	2D-2.5D	um to mm 3D, smooth 3D	0.2um to 10's of microns 3D	New materials, 0.2um to 10's um
NA	0.3	0.5	0.8	1.4	1.4
Micro. Pos.	4	5	1	3	3
Max block area sq	825x825	425x425	285x285 sq	140x140	140x140
Max block diam	1000 (up to 1.7mm dia, IPVisio 15000 speed, 100%, 1.3 power scaling)	600	400	200	200
Min feature size (um)	~2um x,y ~10um z, but freestanding features <20um will deform	~1um x,y ~6um z	~0.6um x,y ~3.3um z	~150nm x,y, ~800nm z	
Min spacing between features um	6-7um (10um recommended)	1um	1um	150nm	
Max feature height (um)	8mm(IPQ)	Thickness of PR	~3mm (IP-S)	~3mm (IP DIP)	~150um (w/170um glass)

Figure 1.2: Nanoscribe Objectives with a quick comparative analysis (Image was taken from official nanoscribe users' manual "Nanoguide" https://support.nanoscribe.com/hc/en-gb/articles/360002996413-Objective-Overview)

$100 \times 100 \times 8$ mm. About 200 nm minimum feature size could be made if appropriate photoresin and objective combination is chosen. As of now, for the minimum feature, the combination of 63x objective and IP-DIP (or IP-DIP2) photoresin is effective. There are 63x, 25x and 10x objectives which are popular for direct laser writing. A number of photoresins are also available in the nanoscribe manual called nanoguide. This is a dynamic platform with the recent updates. But to access nanoguide, one needs to be nanoscribe user.

Figure 1.1 shows different features of different objectives that are used for direct laser writing using nanoscribe. For my thesis, I have used only 63x objective as the minimum feature size desired for my experiments was below 500 nm. In the following section, I am going to discuss about directional coupler and a few relevent literature reviews to utilize direct laser writing in nonlinear integrated photonics.

1.2 Directional Coupler using direct laser writing

Yariv et al. [28] showed a very basic introduction for directional couplers. A directional coupler in optics is a device that allows the controlled transfer of optical power from one waveguide or optical path to another. It plays a crucial role in integrated photonic circuits and optical systems. The basic working principle of an optical directional coupler is similar to that of a traditional RF (radio frequency) directional coupler. It consists of two closely spaced waveguides that are designed to interact with each other. Light is launched into one of the waveguides (referred to as the ”input” waveguide), and a portion of the optical power is coupled to the adjacent waveguide (referred to as the ”output” waveguide) due to the evanescent field interaction between the two waveguides.

At its core, a directional coupler is a waveguide-based structure designed to enable the transfer of optical power between two or more waveguides. The basic principle behind a directional coupler is the coupling of light between two parallel waveguides through evanescent fields – the electromagnetic fields that extend beyond the confines of the waveguide core. This coupling occurs due to the overlap of these evanescent fields when the waveguides are brought into close proximity.

For fiber-chip coupling different forms of coupling have been tried. Son et al. [24] showed different types of coupling between fiber and photonic integrated circuits. Three coupling schemes are commonly used: End-fire coupling, Grating coupling and Adiabatic coupling. End-fire coupling is also known as butt-coupling or edge coupling because of the physical proximity between optical waveguides. There have been studies of fiber pig tailing for semiconductor laser chips [5] [13] [15]. Input and output fiber connection for optical waveguide based modulators was studied by Bulmer et al. [6]. Fiber connections were studied for optical switches [12] [22]. If we focus on the edge coupling for integrated photonic circuit, there have been gradual improvement of coupling efficiencies. Using tapered (large dimension at facet end) waveguide with this edge coupling technique having diffused channel waveguide showed low optical loss [14]. Tapered waveguides having larger facets tend to show low loss as well for polarization dependency and short wavelength [18] [1] [16].

Figure 1.3 shows the mechanism of edge coupling process between a fiber and waveguide of a photonic integrated chip [24]. Let's assume a single mode fiber with E_1 field profile (for simplicity single mode is assumed) and the output waveguide can support multiple guided optical modes where kth mode field is denoted by $E_{2,k}$. Input field E_1 is radiated through the intermediate region of coupling and we name the radiated field E. This E field reaches output waveguide

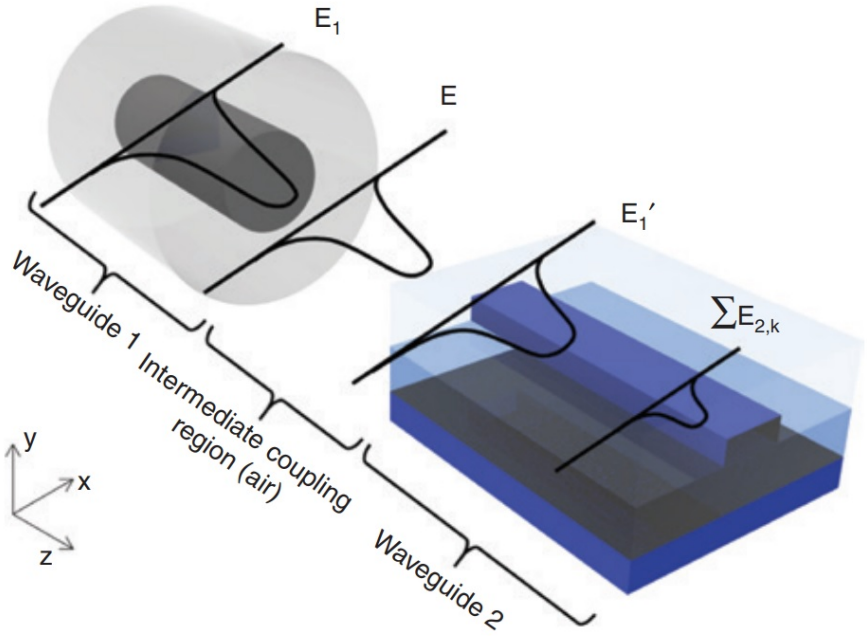

Figure 1.3: Edge Coupling Mechanism [24][This image is taken from this work by Son et al. (2018)]

front facet and the field measured in front of the output waveguide is $E_1{}'$. This $E_1{}'$ field can be coupled to output waveguide's guided modes $\sum \mathrm{E}_{2,k}$. Coupling coefficiency can be calculated from overlap integral of the two modes.

1.3 Direct Laser Writing on Photonic Integrated Circuits

To improve different coupling challenges, direct laser writing has been utilized for 3D integration in different studies. Some of the works have established 3D integration techniques into integrated photonics while some have focused to implement optical phenomena. For nonlinear optics applications, silicon nitride and lithium niobate platforms have been used quite often for 3D integration. Gehring et al. implemented a coupler printed on silicon nitride waveguide which was used for coupling light into chip and extracting the output light [9]. This work was impressive

but due to lower nitride thickness it was not suitable for nonlinear application. Chen et al. showed 3D integration of micro-lenses to improve coupling for photonic integrated circuits with Lithium Niobate platform [7]. Another study showed broadband out of plane coupling using direct laser writing on silicon nitride platform for visible wavelengths [10]. Schumann et al. showed two different examples of implementing 3D polymeric functional devices [23]. One example was a twisting of polymer structure to initiate polarization rotation and the other was to implement a whispering gallery mode resonator connected to silicon nitride waveguide to control coupling to the resonator. Dietrich et al. showed a few beam shaping elements to improve coupling [8]. Power et al. showed a tethered, 3D, compliant grasper which was fabricated on fiber tip [20]. [19].

1.4 Direct Laser Writing on SM fiber

A number of research studies have been done using 3D integration in fiber tip. Hadibrata et al. has implemented metalens in optical fiber tip [11]. Fresnel Rhomb was 3D printed on a fiber tip using direct laser writing by Bertoncini et al. to implement circular polarization [4].Vamol et al. implemented an air-clad taper printed on fiber tip to transmit the fundamental mode adiabatically [26]. Wei et al. demonstrated 3D printed miniature optical-fiber based polymer Fabry-Perot interferometric pressure sensor [27]. Nair et al. implemented fiber sockets based on direct laser writing [19].

Chapter 2: Design of Silicon Nitride-Polymer coupler with 3D Integration on Silicon Nitride Waveguide

2.1 Overview

In the recent few years, a number of approaches were attempted to improve the coupling between a photonic integrated circuit and 3D integrated polymer waveguides using direct laser writing. Also, a lot of free form optics including mirrors and lenses were also tried to utilize total internal reflection, transmission through the polymer material. Photonics chip fabricated at the nanofabrication facility can only facilitate planar lithography to prepare resonators, access waveguide etc. In this way input and output to the photonic integrated circuit is done with edge coupling or grating coupling. Edge coupling has the advantage of ensuring broadband operation. But edge coupling with SM fibers for Silicon nitride devices has a loss of about 5dB/facet. A better choice is lensed fiber which ensures 3dB/facet for the silicon nitride devices. So, interesting designs could be attempted if we can have a better insertion loss and still manage the similar nonlinear optical phenomena that have been established before. The idea is to print couplers on waveguides.In this chapter, the design process would be elaborated for possible nonlinear application. Computer aided design followed by lumerical simulation have found a possible solution if the 3D integration could be performed sensitively. Gehring et al. has implemented

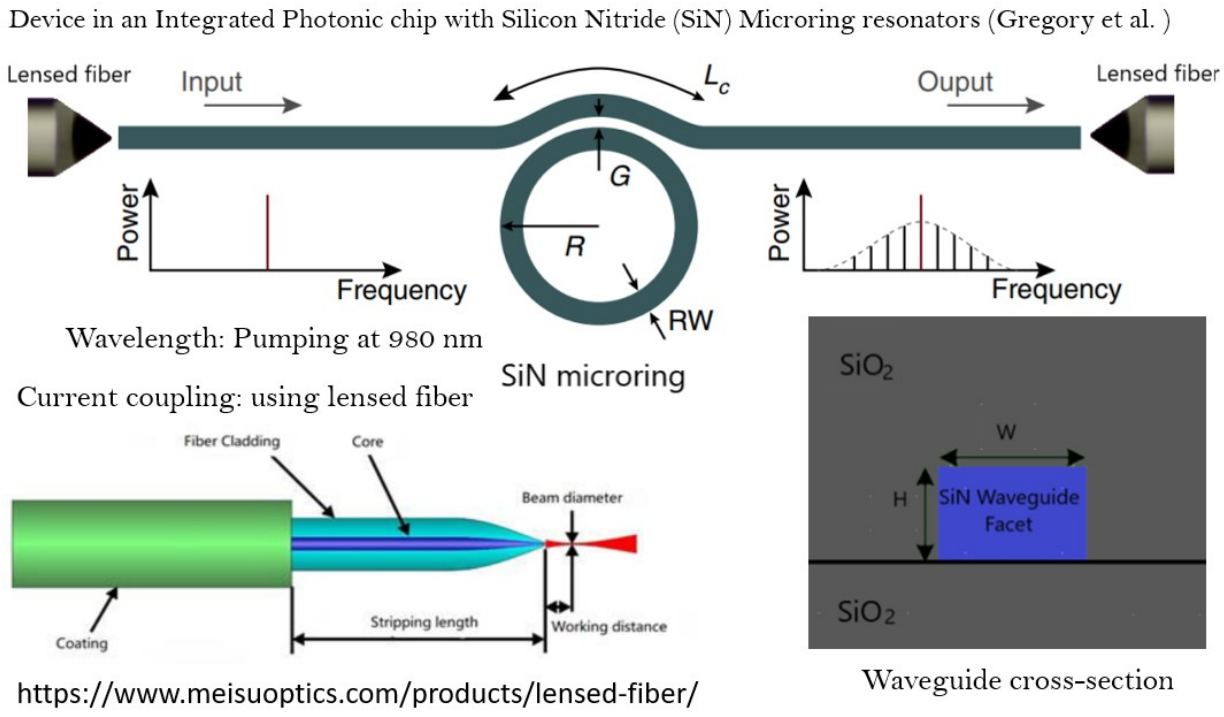

Figure 2.1: Introduction to a common device my group works with: A silicon nitride microring resonator and access waveguide (pully type shown here) is used for nonlinear optical phenomena like frequency comb, optical parametric oscillation etc. Currently we couple laser light (980 nm wavelength for current project) into the waveguide using lensed fiber-based edge coupling that requires a fine polished chip facet. Cross section of the waveguide is also shown in the bottom right. Basic principle of a lensed fiber is shown in the bottom left

an out of plane coupler with silicon nitride being less than 0.5 wavelength thick (1550 nm light and 340 nm thickness of SiN). To improve the coupler for our work where we have about 1 wavelength thick nitride(980 nm light and 420-450 nm SiN thickness) it might be challenging with the evanescent coupling from SiN into Polymer.

2.2 Motivation

Figure 2.1 shows a common device (SiN microring and access waveguide) that is used for non linear optical phenomena like frequency comb, optical parametric oscillation etc. We pump at 980 nm wavelength and the coupling of light is ensured by lensed fiber-based edge coupling

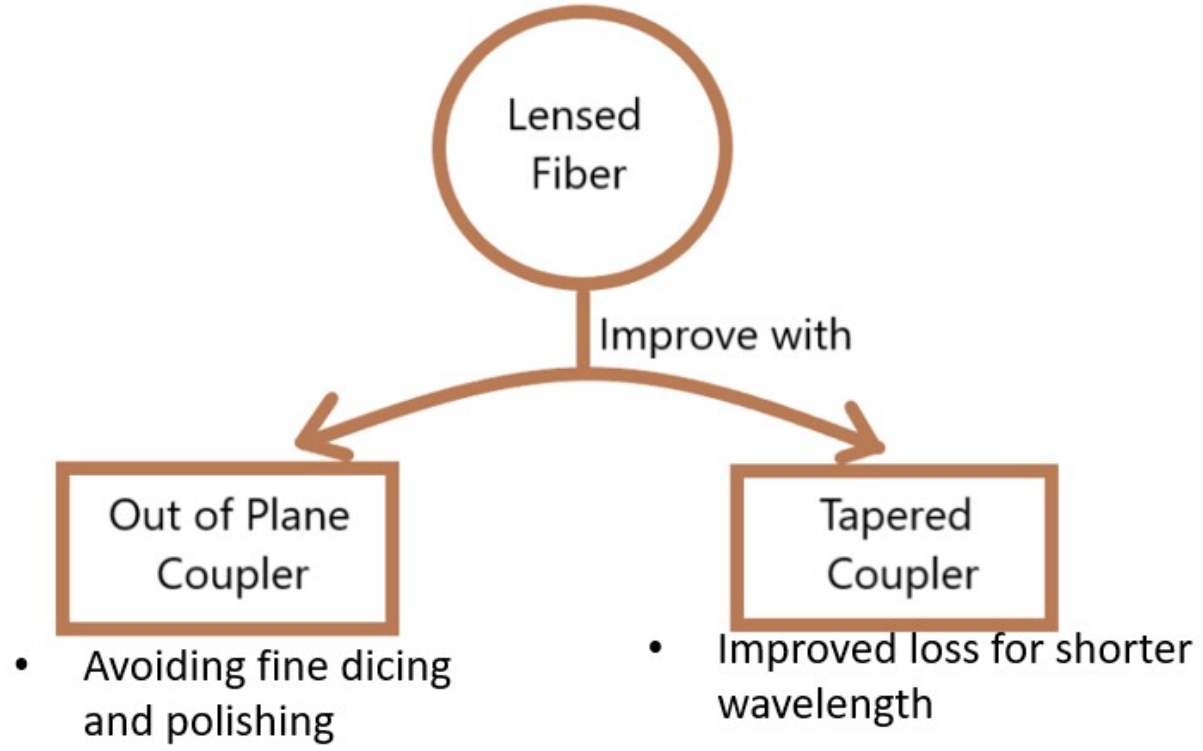

Figure 2.2: Two possible modification to replace lensed fiber: Out of plane coupler printed on waveguide and coupled to SM fiber could be an option; Also tapered coupler printed on SM fiber is another option

which requires a fine polished chip facet. Also, lensed fiber could be fragile and onced the lens get damaged, it might not be reused unlike cleaved fiber. Moreover, we get about 3 dB/facet coupling loss using lensed fiber for our devices. So there are scopes to improve the coupling mechanism specially for shorter wavelength as modes are very confined at shorter wavelength. To avoid polished facet part and to improve coupling at shorter wavelength, the proposed two coupling mechanisms (Figure 2.2) could be useful for nonlinear integrated photonics. Chapter 2 will be about the out of plane coupler and the following chapter will discuss the tapered coupler.

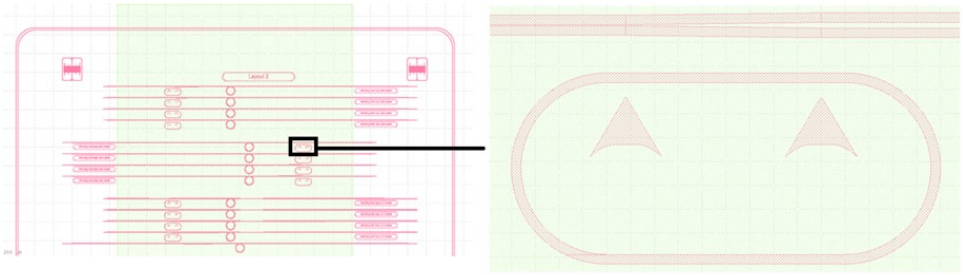

Figure 2.3: The layout was prepared using CNST Nanolithography toolbox [3]. It contains access waveguide and microring devices, the geometry of which has been finalized by dispersion simulation. The selected portion is zoomed that shows the downtapering of SiN marked by the arrowhead alignments. This is the region where we start to print the out of plane coupler.

2.3 Chip Layout for 3D integration

Before aiming for the 3D integration using nanoscribe tool, we need to have a photonic integrated circuit in hand. So chip layout design is the first step for this. Prior dispersion simulation parameters were used for the geometry of ring resonators and access waveguides. These geometry numbers were used so that it could be used for nonlinear optics right away once the silicon nitride-polymer coupler works. The ring radius 23 micron, waveguide width 550 nm, ring width 850 and 950 nm, gap between ring and access waveguide 200 and 250 nm. However, 550 nm waveguide width was up-tapered to 1200 nm and over 41 micron length it was tapered down to 200 nm. This 41 micron length is the coupling length for the 3D integration. To find this 41 micron region, layout has two arrowheads pointing to the two points as aligning support. The layout design has a few blocks tweaking the gap and ring width of the ring resonator. This layout was generated using CNST Nanolithography toolbox and was fabricated accordingly.

Figure 2.3 zooms the section in the photonic integrated circuit layout where 3D integration would be implemented.Figure 2.4 elaborates the printing region for 3D integration.

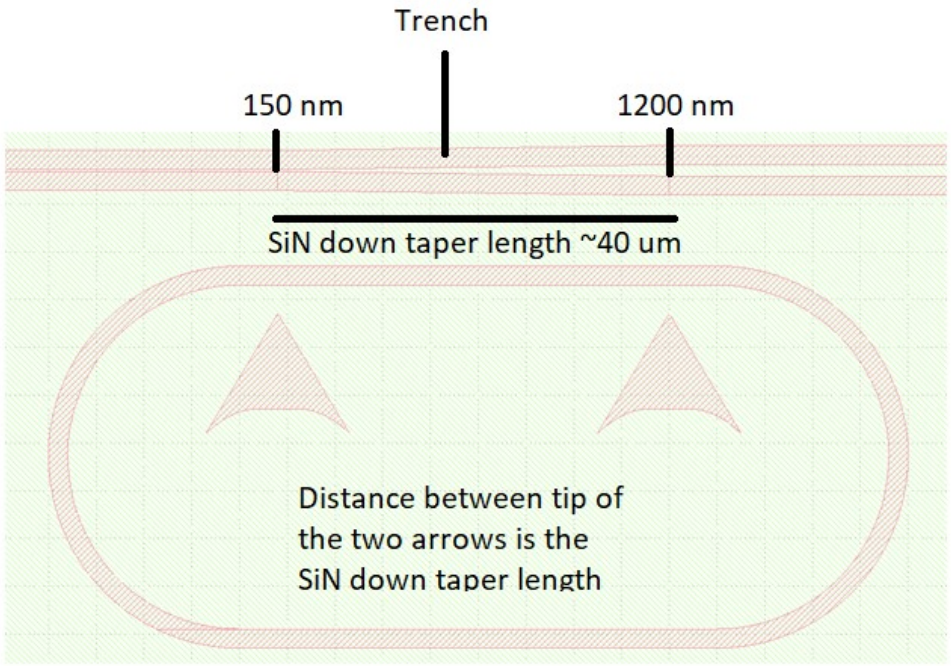

Figure 2.4: Printing region showed in details: Before downtapering starts, SiN waveguide width is 1200 nm and over 40 μm of length it gets downtapered to 150 nm. After that, it continues as a straight section for about 60 μm just to stay as a bottom support for the polymer coupler

2.4 Computer Aided Design for the Polymer coupler

Gehring et al. showed a polymer coupler on silicon nitride waveguide but that structure was not suitable for non linear optics application due to lower thickness of nitride. Nominal thickness of 420-450 nm Silicon nitride wafers were available for this work and a prior lumerical simulation was done to tweak the coupling length, height of the polymer coupler with a constant 2 μm width. Ideally a height tapering of the polymer from 0 to 2 micron is suitable choice. After this region that is supposed to be printed on the coupling length, the polymer waveguide takes a bending. For this purpose, Gehring et al. chose to make a tilted coupler and created a setup to extract light from the tilted coupler. One possible trial version was made with tilted coupler as shown in Figure 2.5. In this design, the vertical height was carefully chosen so that the fiber that

would come close to the tilted part, does not hit the chip surface. A sample image from scanning electron microscopy is shown in the Figure 2.6.

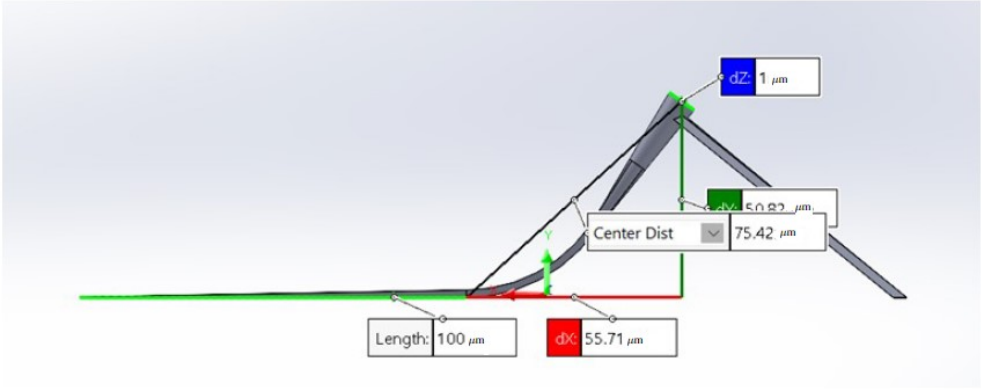

Figure 2.5: Tilted polymer coupler design (No lens at the output). Designs were prepared in solidworks. 100 μm length shown in the figure corresponds to the height tapering of the polymer waveguide that sits on top of the downtapered SiN waveguide.

In the next section with Lumerical simulation, this height tapering of the polymer would be focused. However, since usual optical experiment includes a horizontal fiber placed in a fiber holder, an alternate design was made so that horizontal SM fiber can reach the horizontal output part for the light extraction. This design would require a S-bend along with a bit stronger mechanical support to ensure the structure sticks. Figure 2.7 shows the design with segmented part introduction.

2.5 Simulation of the Structure

Using Lumerical Mode Solution and FDTD, different sections were simulated to verify the device performance. The total polymer structure could be divided into three parts-Coupling region, Bending region and output taper region.

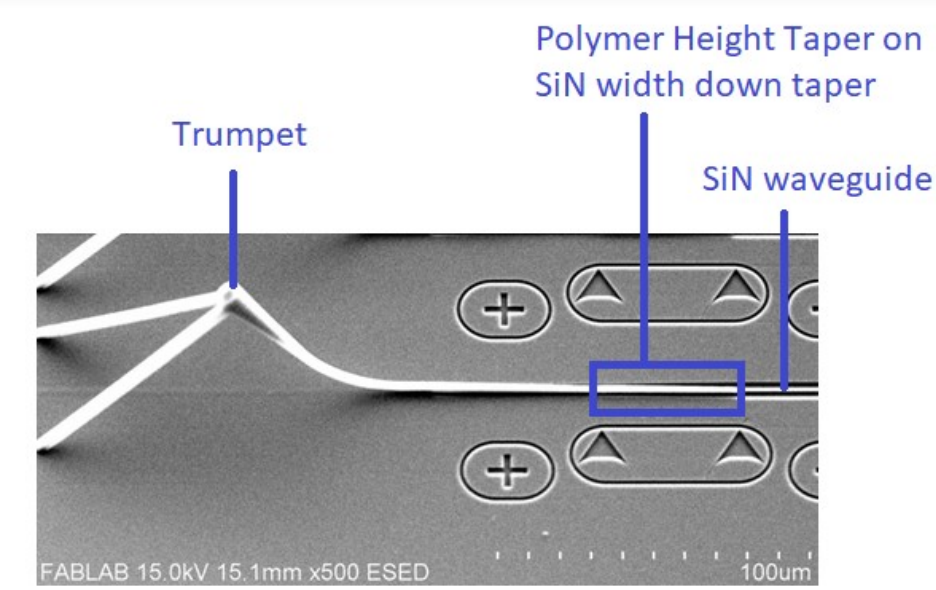

Figure 2.6: A Tilted Polymer coupler (Trumpet) on SiN waveguide. The blue labelling denotes a few important parts. These couplers are designed to be integrated on top of the SiN waveguide which is labelled, and it gets down tapered between the two arrowhead alignment markers. In the same downtapering length, Polymer waveguide gets a height tapering and then bends and tapers up. These couplers also need mechanical support as we see two tethers near the circular top. The basic concept of this structure is evanescent coupling would take place from SiN into polymer followed by mode expansion and collimation will take place.

2.5.1 Silicon Nitride-Polymer Coupling Region

There are a few important sections of simulations which start with the Silicon nitride-Polymer coupling region. Silicon nitride waveguide width needs to be tapered down and the thickness of the polymer waveguide needs to be tapered up in height with a constant width.

SiN chip layout includes 23 μm radius ring and 850 nm, gap between ring and access waveguide 250 nm. Access waveguide width is 550 nm and it gets tapered to 1200nm and downtapered to 150 nm over 41 μm taper length followed by 60 μm length with constant 150 nm width. Figure 2.8 shows the optimum 41 μm taper length. Simulation of this section for light coupling between nitride and polymer is as follows (980 nm light) in Figure 2.9. The field

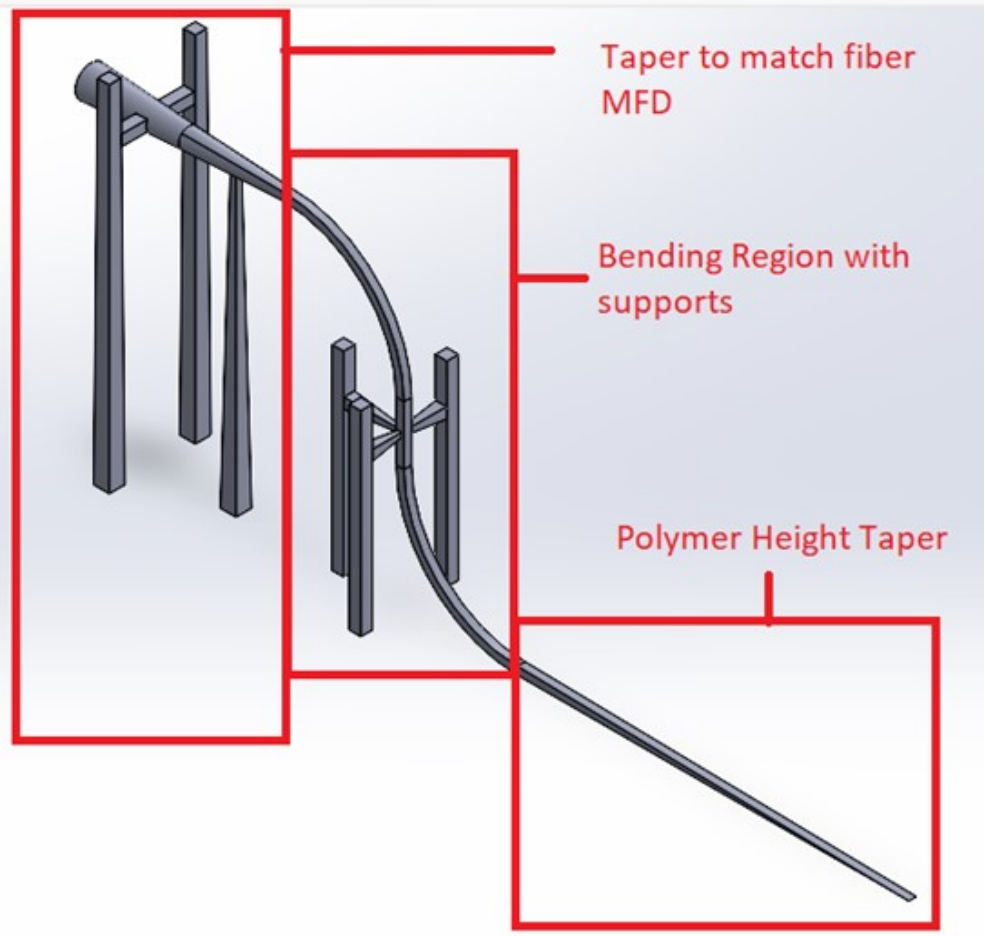

Figure 2.7: Computer-aided design of the polymer coupler-three region blocks are simulated separately since total structure simulation is computationally intensive. The regions are: polymer height taper (Evanescent coupling region, bending region and fiber matched taper region)

propagation shows that after about x= 60 micron position, light gets into polymer and no light is in nitride anymore although the nitride is still present with the constant thickness but reduced width. A slight scattering into the substrate is visible but that does not make the simulation result very bad.

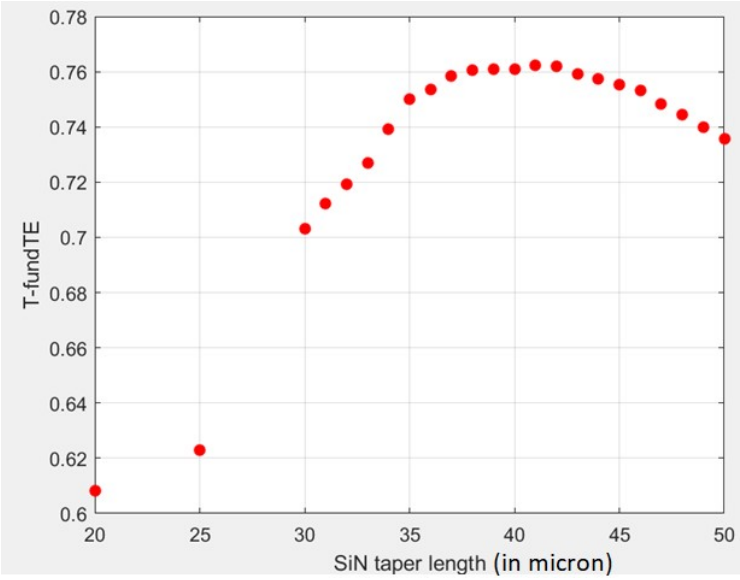

Figure 2.8: Fundamental modal transmission from SiN into Polymer. The down taper length was varied to check the optimized taper length in terms of fundamental TE modal transmission. Optimized taper length was 41 micron for 980 nm light.

2.5.2 Bending Region

When the polymer coupler height tapering is done on top of the SiN down taper, it starts to bend. Pernice group tried the bend followed by taper to couple light such that it becomes a tilted structure. My design includes the bend like an S bend and get horizontal and tapered up to MFD matching diameter to couple to fiber.

S bend loss is quite low if the bending radius is about 25 μm. For a 2 μm x 2 μm cross-section S bend, Transmission for modal TE is about 98 percent without any support. Adding the supports for mechanical stability add very slight scattering loss and with 2 supports in the S bend region causes the modal transmission to be about 92 percent. So overall the S bending region is working. For the support dimensions, a few quick simulations were done which summarize that the support should be touching the bending polymer at about 1 μm x 1 μm cross-section and the supports would be tapered up towards the bulk nitride chip surface.Figure 2.10 shows

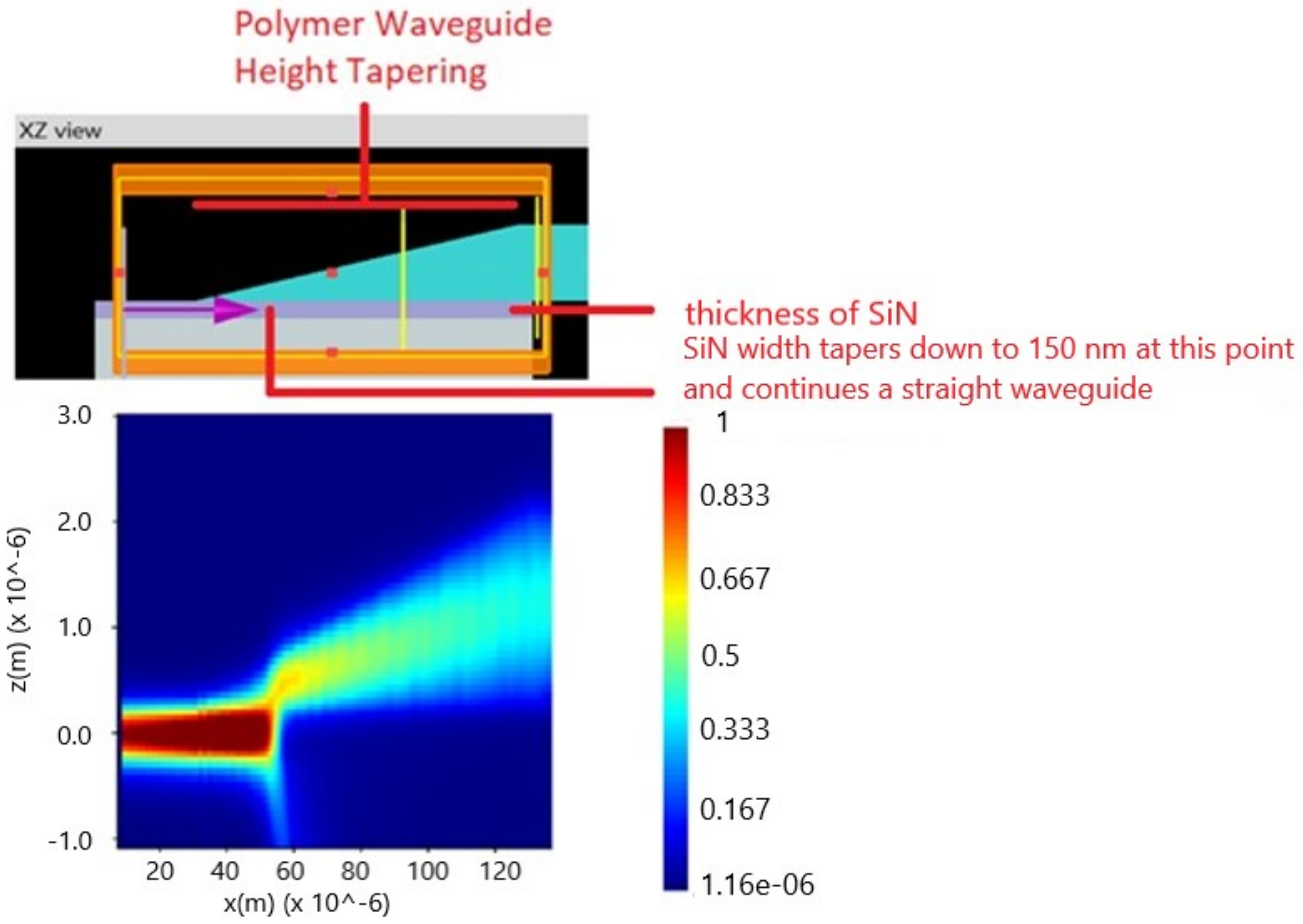

Figure 2.9: Schematic of the design and the field propagation of SiN-polymer in Lumerical FDTD: The orange rectangle denotes the simulation region; This image only shows change of heights therefore the nitride thickness is constant and polymer on top of the downtapered nitride width is seen to have a tapering height. The bottom figure shows the field intensity of light entering the polymer

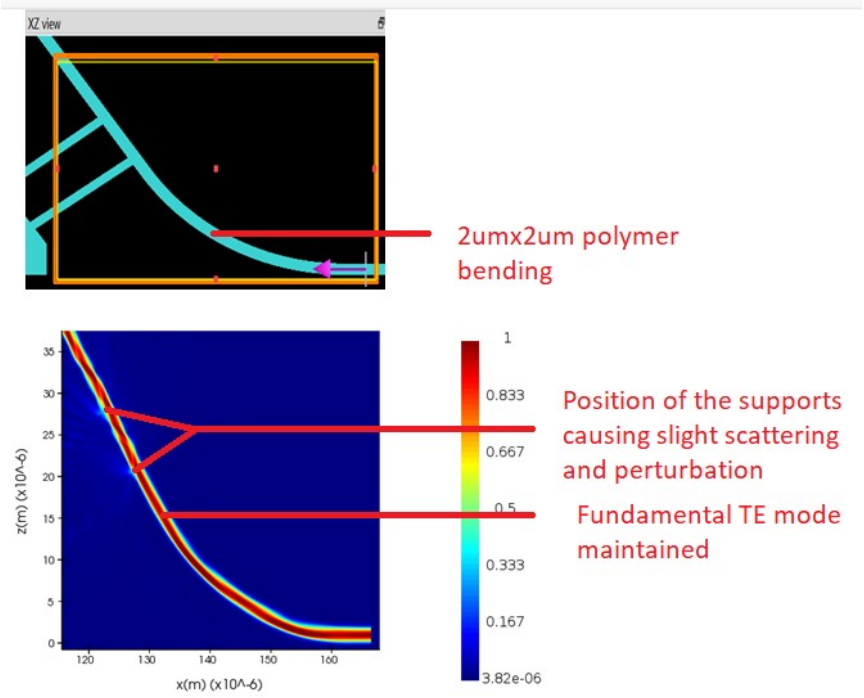

Figure 2.10: 45 degree Bending region maintaining fundamental mode. Slight Scattering loss is visible at the contact point for the supports. Support loss has been simulated to be about 0.3% per tether

the propagation of light in the bending region. A slight scattering is seen when light reaches the support positions, but eventually TE mode is maintained as the gaussian field profile was visible.

2.5.3 Polymer Coupler-SM980 fiber coupling

FDTD mode solution simulation shows that 8 μm diameter of the coupler has the maximum overlap with SM980 fiber based on MFD matching. It requires the bending region end cross section of 2 μm x 2 μm to transform into 8 μm diameter (Circular). The tapering needs to be adiabatic over 100 μm length. Figure 2.11 shows that if sub micron diameters could be reached, it could still give near 80% overlap between SM980 fiber and polymer coupler (the horizontal part). However, althought this could ensure single mode, it also has physical instability due to this small dimension and the support to keep them working would have substantial perturbation. Therefore,

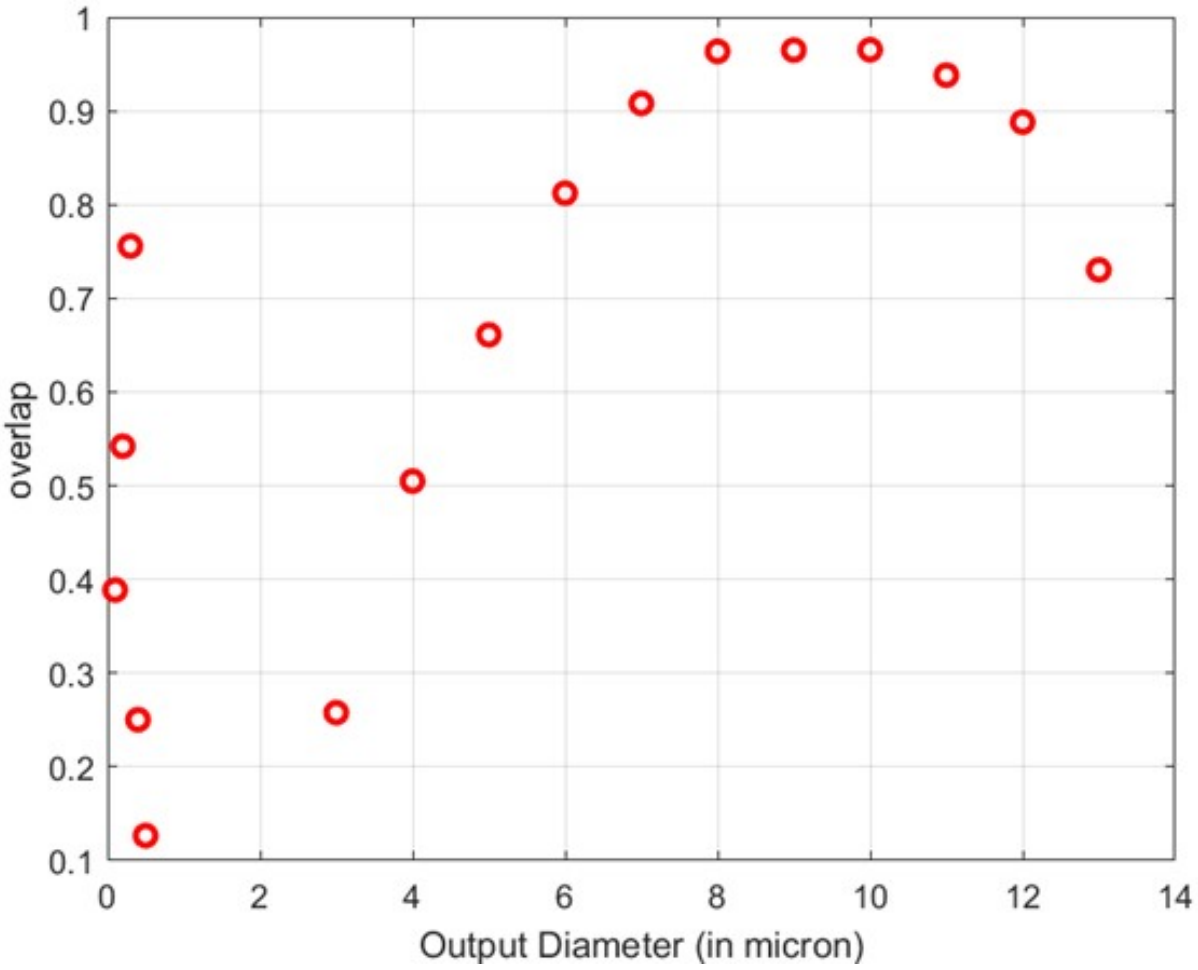

Figure 2.11: Optimized output diameter with maximum overlap between SM980 fiber and polymer coupler (Optimized 8 um)

a safer option is to choose 8 micron diameter. The challenge here is this larger diameter can have multimodes and thus making it adiabatic is the goal. That is why 100 micron taper length is sufficient to make it adiabatic with good efficiency.

2.6 Dose Testing for the Polymer Coupler on Silicon Nitride

For any fabrication, dose testing parameters are sensitive. Unlike the nanofabrication dose parameters, direct laser writing also needs a few dose parameters. These parameters include but

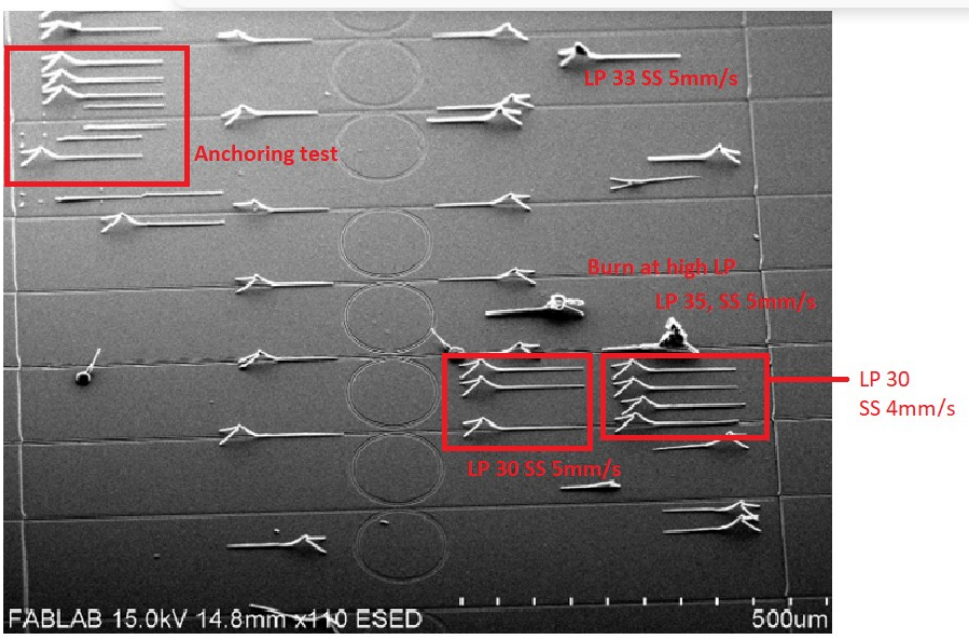

Figure 2.12: Dose impact: Dose testing were done in multiple steps. This is a summary of that. Laser power was varied from 25 to 35% and Scan speed was varied from 3 to 7 mm/s. Percent of laser power follows the reference of 50mW average power at 100% laser power. Dose testing also needed anchoring for the mechanical stability. Anchoring means adjusting the z-offset to start printing for sticking structures. A successful print might force the print to start a little bit inside of silicon nitride instead of printing exactly on top of SiN waveguide taper.

not limited to laser power (LP), scan speed (SS) (galvo/piezo/stage), slicing layers, slicing and hatching distance etc. Dose testing is also sensitive with the aging of the photoresins. Challenges with dose testing include stability of the printed CAD design, maintaining the design parameters, anchoring (adjusting z offset for printing) etc. Sometimes a lot of structures do not stick due to wrong laser power-scan speed combination. High laser power might cause burn while lower laser power might not print suitably for not having cross-linking.

I started with the tilted coupler. First approach was done on a 1inch by 1 inch fused silica slide. Glass slide was just a starting point to check if a suitable dose could be found. With IP-DIP photoresin and 63x objective, 30% laser power and 4mm/s galvo scanspeed was a suitable combination for glass slide. The next challenge was to print on photonic integrated circuit. Figure

2.13 shows the printing of the tilted couplers on top of waveguide. This was a print to test the stability and there was no careful fixed position to print.The structures were standing. So the next step was to print them in a fixed place where SiN waveguide was tapered down. Since the 3D integration needs to be done on the Silicon Nitride waveguide on 41 micron length, first challenge is to find the devices in the nanoscribe microscope. Then using the stage movement, cross-heir and laser spot need to be aligned manually and find the starting point using the arrowhead aligners. Figure 2.12 shows the dosing impact. Dose testing is sensitive because if the we do not have the suitable condition, there might be issues like bending, burning or improper print with mismatched parameters. In this figure, a few regions are shown where we have structures that fell as well as nicely standing structures. A few burning cases are also visible. So, after this dose testing, the most optimized laser power and scan speed combination was chosen.

2.7 Anchoring Challenge

Anchoring is the most challenging part of this 3D integration. Anchoring means finding the exact z height to start printing. For the printing air clad region needs to find in the nanoscribe microscope. It is not done using autofocus as it might damage the chip since it is patterned. Manually the devices in the air clad region are found. Find interface option always brings into the Si/SiO2 interface as it has higher refractive index. Over 3-micron thickness and 450 nm thickness of nitride print needs to be started. So roughly 3.45 μm needs to be adjusted from finding the focus to get into the right interface. The anchoring test found adjustment of 4.3 μm works. Figure 2.14 shows a few unwanted scenario of bending and broken structure for not being anchored properly. Figure 2.15 shows another case of distorted shape where the starting point

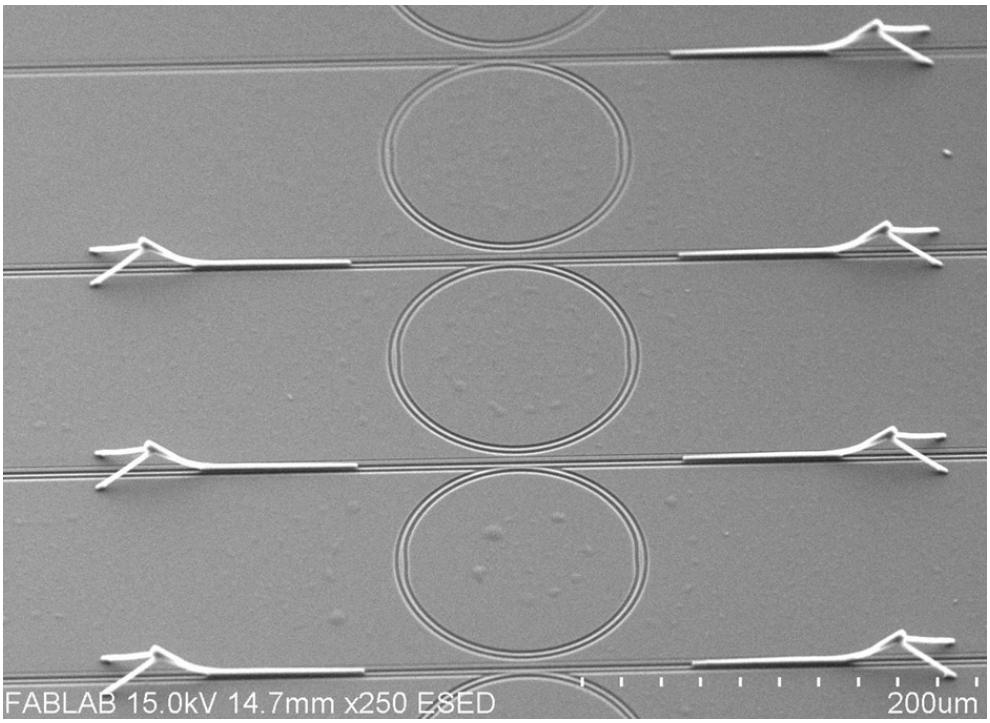

Figure 2.13: LP 30, SS 5mm/s dose seems to be working great. These prints were done to test the mechanical stability of the design by Pernice group [9]. Also, these were printed on top of a fixed width waveguide (550 nm). Optically this print would not work as SiN has not been tapered down. So, light would not pass into polymer.

seems to be misaligned. It was noticed if the z offset is chosen precisely, this does not happen.

2.8 SEM Imaging of the Couplers

Any print using nanoscribe needs SEM image to justify its feasibility. Sometimes wrong dose makes the structure dimension wrong. Without doing SEM image it is tough to decide which the right combination is. A few SEM images are shown here in Figure 2.16 and Figure 2.17.

2.9 Alignment of the coupler

Printing alignment of the polymer on top of SiN waveguide needs to be fine with reference to SiN waveguide. The following Figure 2.18 shows good alignment although done manually.

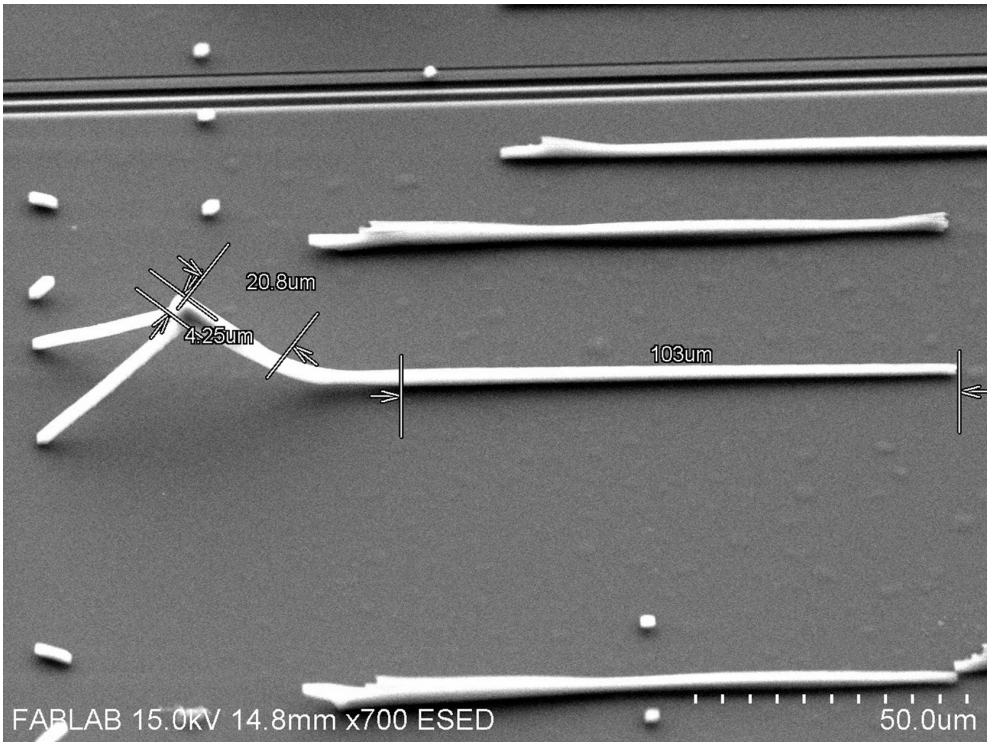

Figure 2.14: 100 μm polymer taper bends and gives incorrect dimension as well (Not designed case). It shows that with an incorrect z-offset for anchoring, structures could also be broken or washed away

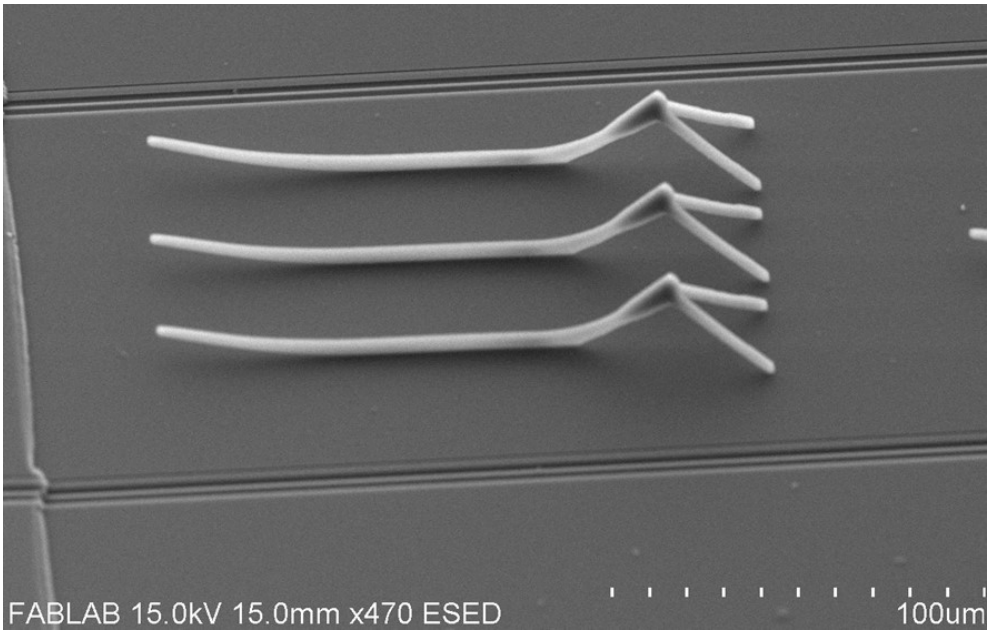

Figure 2.15: Incorrect Anchoring causes distorted shapes. The height tapering part is no longer attached to bulk nitride rather moved away. These prints are attempted on bulk nitride to check their adhesion.

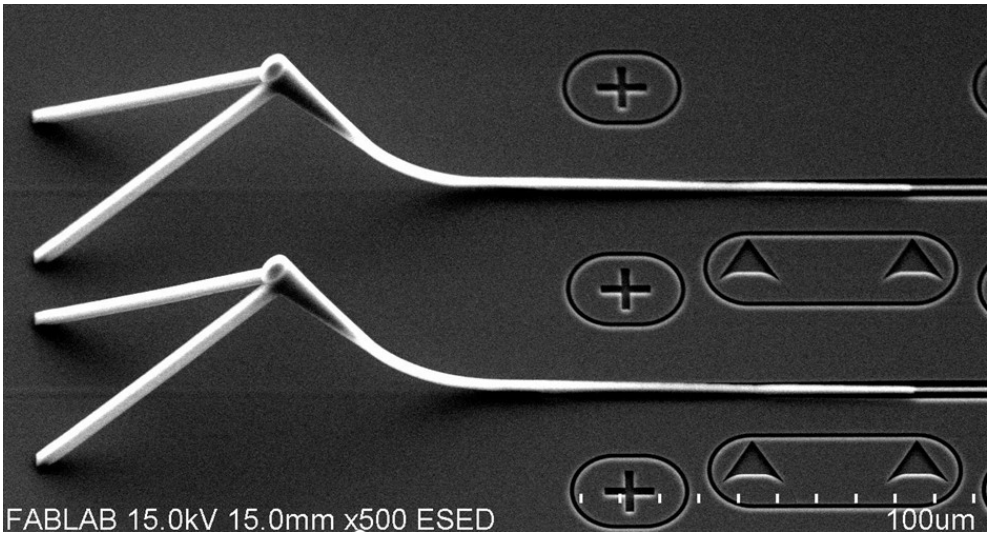

Figure 2.16: SEM of the tilted couplers on chip with alignment

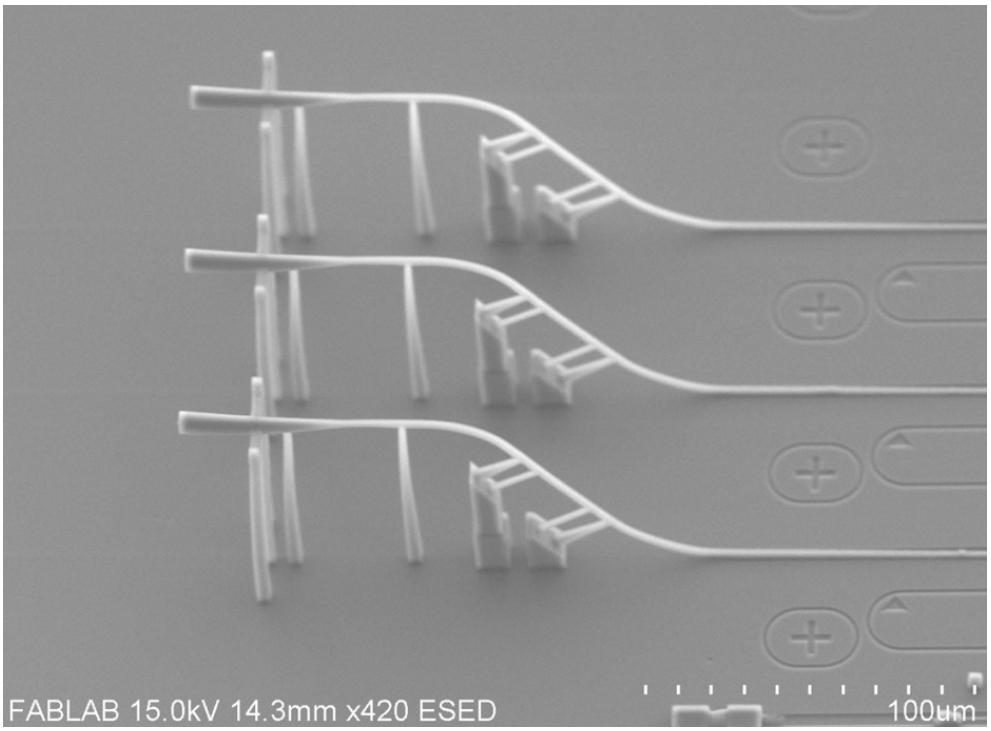

Figure 2.17: Modified horizontal couplers: Clearly better support system is needed compared to tilted case

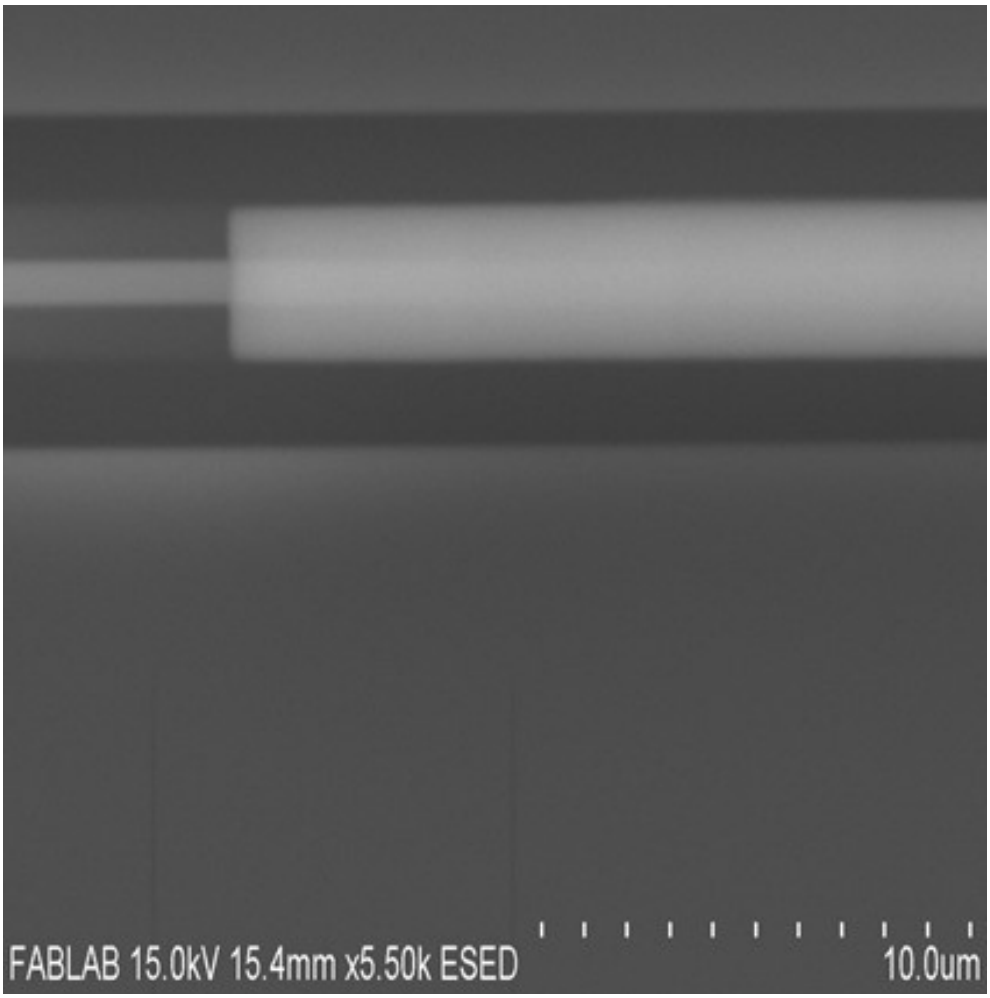

Figure 2.18: SEM of the alignment: thin white in the middle is the SiN waveguide and on top of it the thicker white part is the polymer coupler. With manual alignment and proper anchoring, this could be achieved

Manual Alignment: First, devices need to be in good focus inside nanoscribe microscope. This is easily done by focusing the microring and access waveguide. Then the printing region is focused with some zoom. The trench region (black) and white region (waveguide) is visible. The best possible zoom is done on the waveguide region of printing interest. The middle point of the waveguide is found manually moving the stage of the nanoscribe tool. Stage can move 100 nm minimum. Figure 2.19 shows the point where direct laser writing is started. This point is also detected from the arrowhead marker in the bottom.

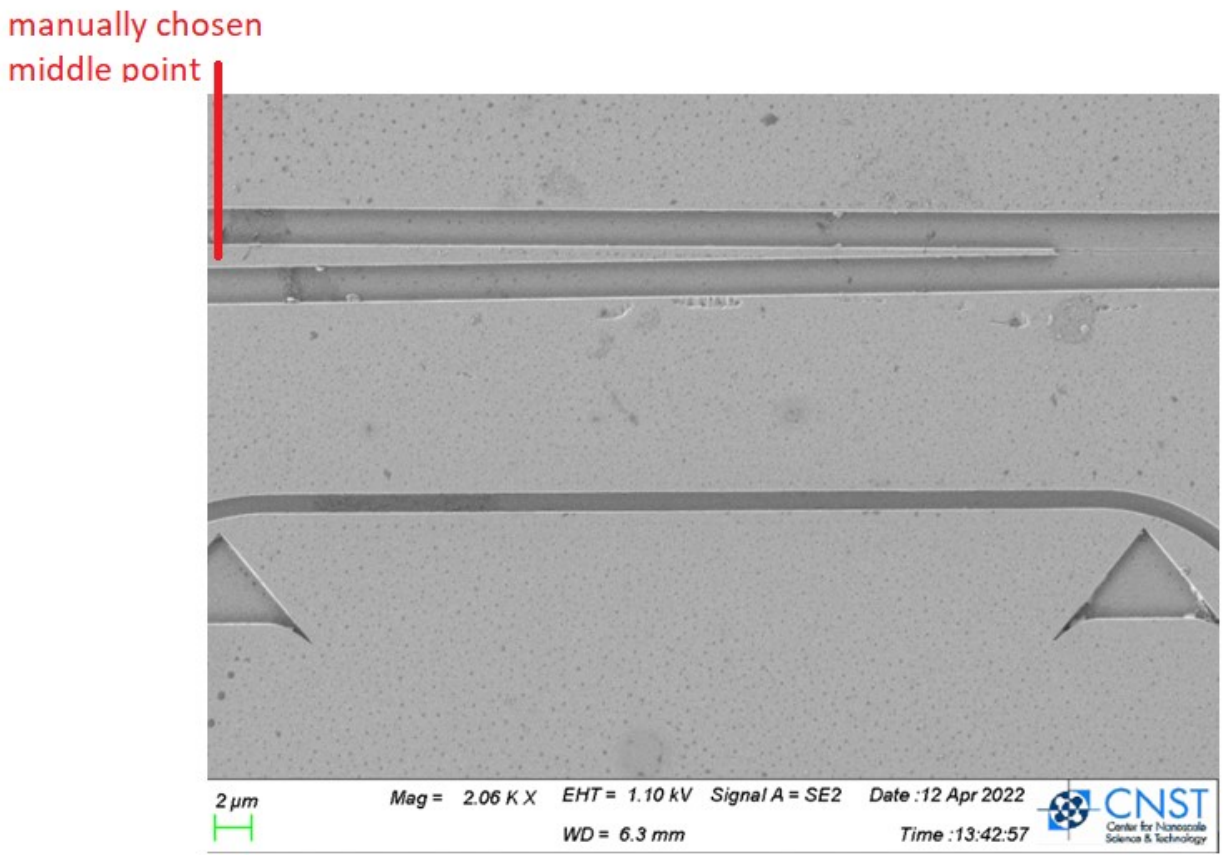

Figure 2.19: The point we choose as the middle point of the waveguide is shown. It refers to the arrowhead marker. Same process is done on the other arrowhead marker.

However, it is sometimes tough to be precise to find the middle of the waveguide. To print the couplers we need to set an x axis for printing, and we do it by choosing two points of the waveguide. Basically, two middle points at two different locations (preferably these two locations are chosen by the arrowhead alignment marker). Things get tougher because it is hard to make the waveguide exactly horizontal in the display. So, the best we can do to make the polymer coupler aligned to it is to ensure the printing x axis is parallel to the waveguide. There is a greater likelihood it would not be perfect most of the time unless some automatizing is done. Figure 2.20 shows an imperfect alignment which could lead to higher coupling loss.

Selected 7 samples' deviation from the waveguide middle is shown here using the SEM

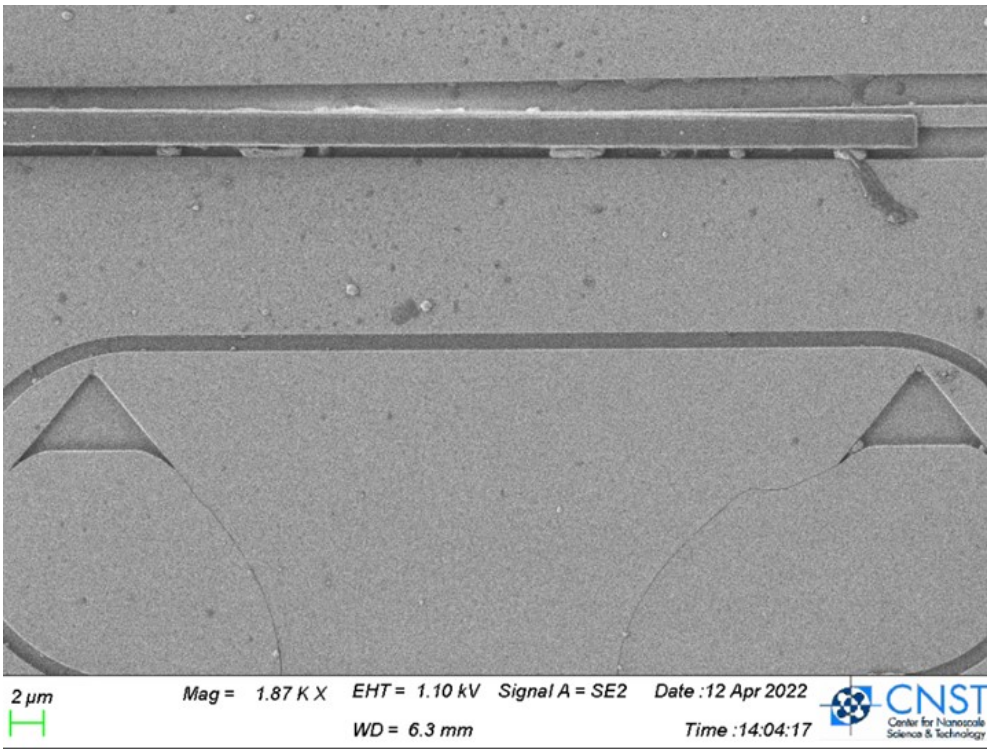

Figure 2.20: An alignment case where an offset angle is visible following the manual process described. Clearly the two middle points were not chosen in a precise way which is adding the angle between polymer and SiN waveguide.

scalebar roughly. This manual process might vary from person to person to find the axis precisely. Alignment error can occur in two ways: First, the structure could have a vertical shift based on the chosen middle point manually and second, it can start printing at a slight angle due to not choosing the axes perfectly. Figure 2.21 shows the sample deviations.

2.10 Machined Piece in Setup

An aluminium based metal piece was machined to place the photonic chip. It was done from terrapinworks UMD. This piece is screwed in a stage so that it could be moved. Figure 2.22 shows the machined piece, that was used.

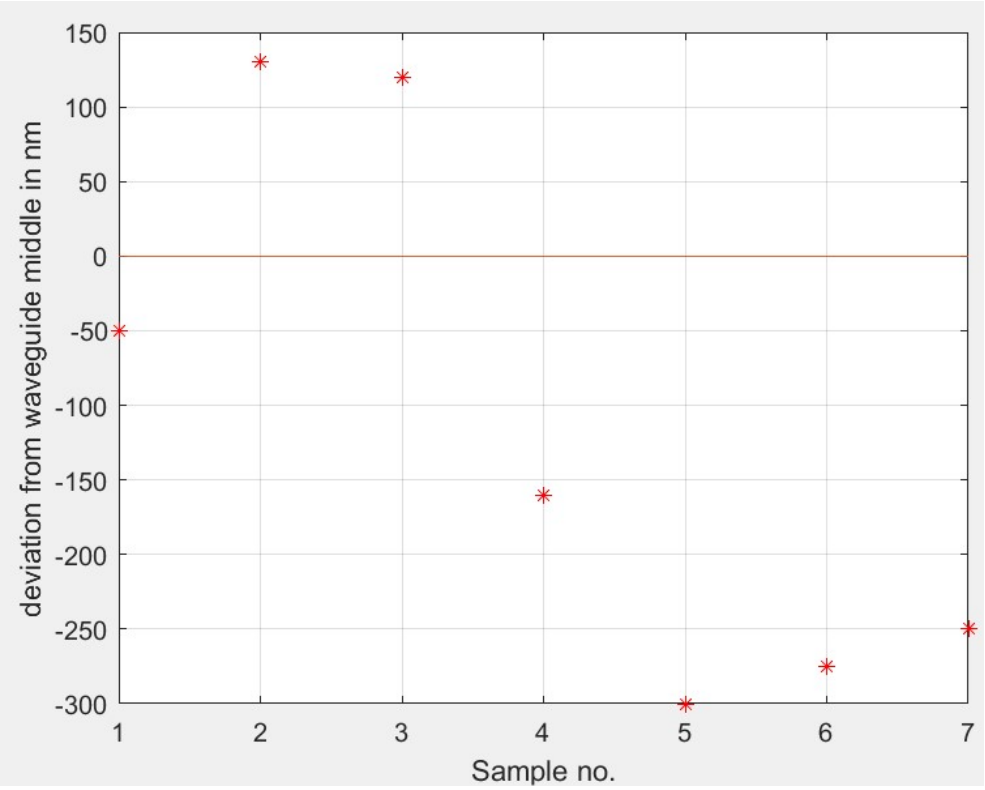

Figure 2.21: Deviation from the middle of the waveguide is quantified for 7 samples. Positive value denotes that the polymer axis is vertically up-shifted with respect to waveguide axis and negative value denotes the opposite.

2.11 Experimental Measures

Although simulation showed promising results, but in terms of experiments, coupling (about 18 dB loss) into polymer from nitride was poor. This could happen from a few reasons:

-Cracked nitride chip with wrong dimenstion in the tapering region (before nanoscribe)

- Anchoring might ensure the structure sticking but it someway included the coupler a little bit inside the SiN waveguide instead of staying exactly on top of SiN waveguide

-Touching the bulk nitride cause huge loss

Figure 2.23 shows the scattering of light causing very little light at the output.

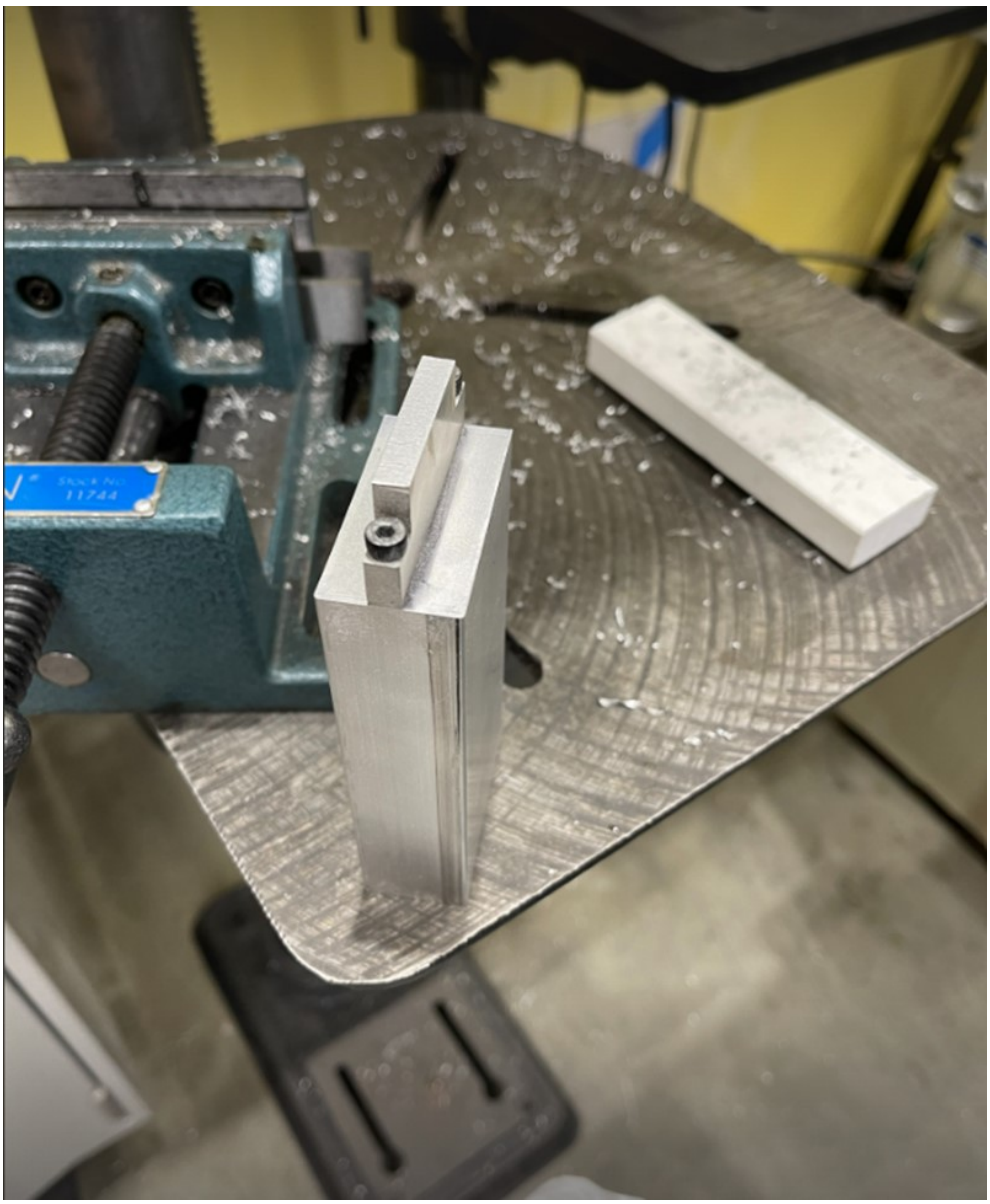

Figure 2.22: UMD Terrapinworks did this Machined piece to place the chip. The reason to machine this is to adjust the height in the experiment setup.

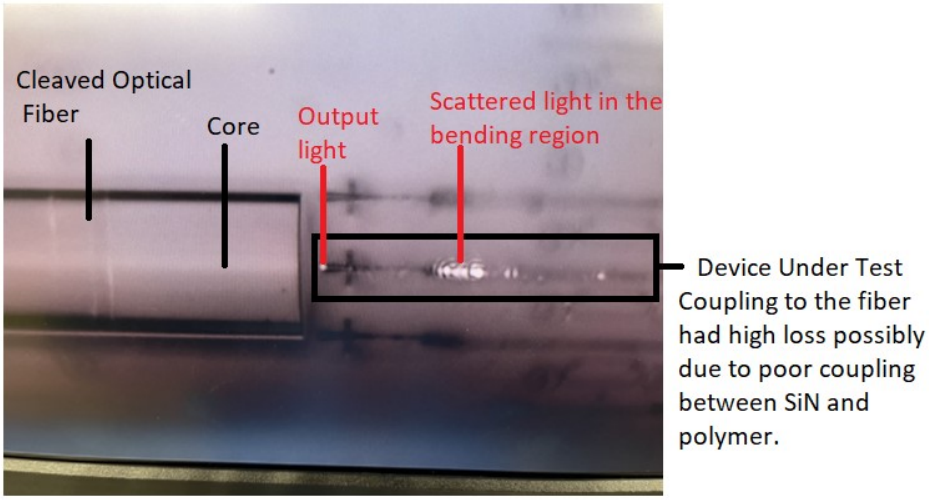

Figure 2.23: Experimental Measure: due to poor coupling between SiN and polymer, enough light do not reach the trumpet output to couple with SM fiber. The coupling loss is about 18 dB which is due to insufficient coupling from SiN into polymer waveguide and the middle shiny scattering region denotes that light is scattered on the bending region support instead of fully coupled into polymer waveguide

2.12 Improper devices

Figure 2.24 shows mismatch of fabrication with respect to design. Tapered SiN was expected in between the two arrowhead markers but clearly the tapering terminated before the desired length. After the tapering down, the SiN width we expect is 150 nm but due to early termination (Figure 2.25), the width is about 227nm. If the 3D integration is perfectly done on top of waveguide, 227 nm width would give about 25 percent transmission of the fundamental modal TE transmission which correspond to a 6 dB loss.

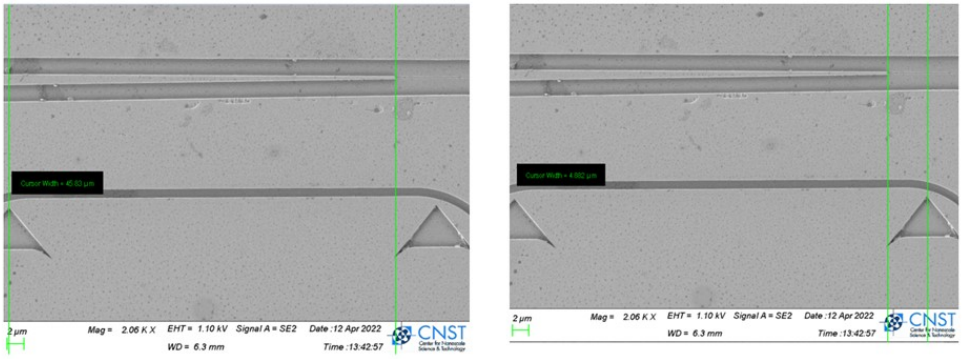

Figure 2.24: Cracked Nitride impact: about 90 percent of tapered length is written

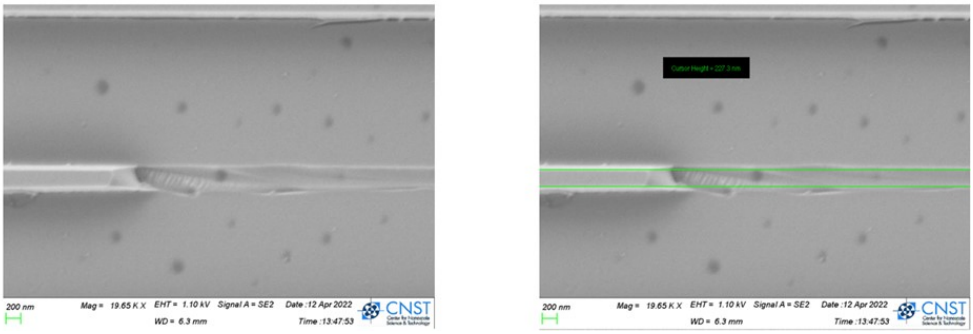

Figure 2.25: The part that is broken is zoomed: final width is about 227 nm whereas our design was for 150 nm.

Chapter 3: 3D integration of Truncated cones on SM fiber

3.1 Overview

Single mode (SM) fibers are used for edge coupling to couple laser light into the waveguide of photonic integrated circuit. Lensed fibers are widely used for edge coupling which provide about 3dB/facet loss for our group's silicon nitride resonator-access waveguides and suitable for the nonlinear phenomena like frequency comb, optical parametric oscillation etc. Also lensed fibers do not require to be extremely close to waveguide for coupling rather the best coupling happens when there is a gap between lensed fiber and chip. Single mode fibers, on the contrary, could still couple after cleaving the fiber but the insertion loss is roughly 5 dB/facet causing higher optical insertion loss and it needs to be placed quite close to the chip with a possibility of chip facet damaging by touching the SM fiber(butt-coupling). However, 3D integration of cone couplers printed in the core of the SM fibers could give equivalent or better performance than lensed fibers as per simulated structures. Concept of polymer cone coupler is simple. It is a down-taper structure with circular cross-section at both end. This coupler printing starts at the SMF core to ensure mode matching. The MFD matching is ensured. Then we have a down tapering region. At the chip side of the down-taper structure, the polymer core should be mode-matched with the desired photonic integrated circuit mode profile. Provided this is a possible option fabrication wise using nanoscribe direct laser writing, it could be a suitable

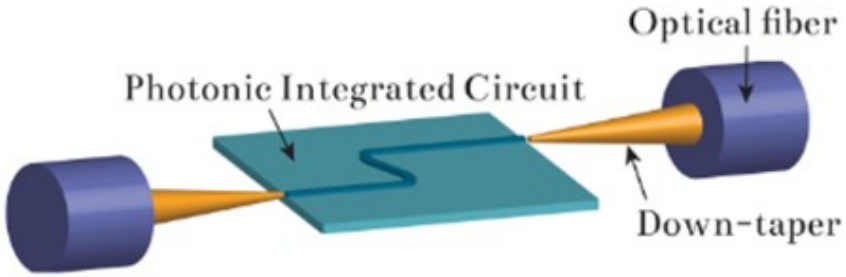

Figure 3.1: Cone Coupler (Orange color) Concept [25] [The image is taken from Vanmol et al. (2020) work to show the design]

replacement for lensed fibers which are costlier than SM fiber. Vanmol et al. [25] has worked on these couplers and showed that for 1550 nm light using Silicon nitride waveguide (About 1 μm width and 400 nm thick) this coupler can give coupling loss of 1.65 dB whereas lensed fiber gives 2.09 dB loss. They also tried for Si (250 nm x 250 nm), SiON(4 μm x 2.5 μm) and InP(2 μm x 1.5 μm) waveguides and got 2.69 dB, 1.34 dB, 4.18dB loss with the couplers. For our group's work shorter wavelength based nonlinear optics could also be made possible using these couplers. Design of the couplers need to be engineered and that is why this could be interesting.

3.2 Fiber Preparation

3.2.1 Introduction to SM Fibers

Single mode (SM) fibers have a general structure irrespective of the wavelength. This has four parts: Jacket, Buffer/Coating, Cladding and Core. When we see the yellow 3mm jacket, we use fiber stripper to reach the 125 μm cladding layer which is the minimum we can reach. Then using nanoscribe microscope we must find the core region and align the designed cone with the core.

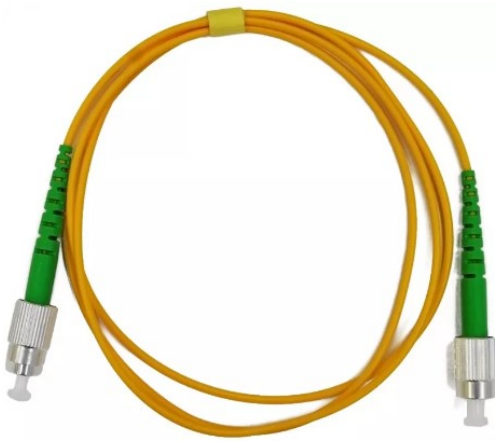

Figure 3.2: A Sample SM fiber with the yellow jacket

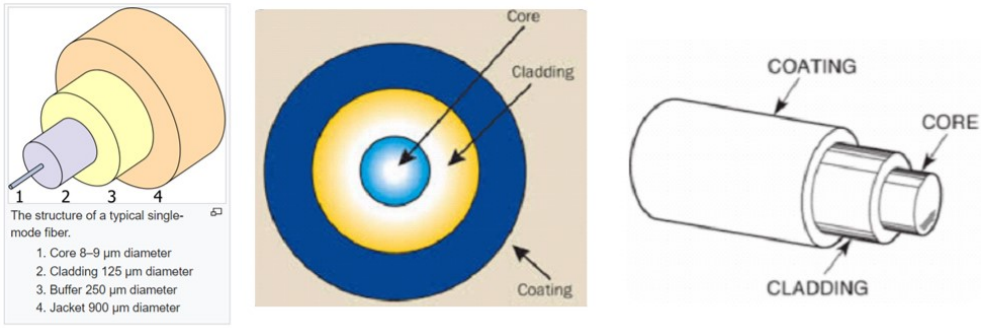

Figure 3.3: Structure of SM fiber shown from Wikipedia image followed by core and cladding from top view(https://en.wikipedia.org/wiki/Core_%28optical_$fiber$%29)

Figure 3.2 shows a SM-980 fiber with yellow jacket. In order to use direct laser writing on SM fiber, a step-by-step process is followed. After the jacket, there is 250 micron buffer followed by 125 micron cladding layer. This cladding layer is the best we can reach after stripping. Different portion of an SM fiber is shown in Figure 3.3.

3.3 Fiber Preparation

This section shows the stripping details.I used a fiber stripping tool to reach the 125 μm cladding layer that we would work with in the nanoscribe tool. Figure 3.4 shows the cleaving tool.Since I required a very nice cleaving, I had to use the cleaving tool after the stripper was used.

Figure 3.4: Fiber Stripping Tool

Another challenge was to ensure a cleaved length as minimum as possible. Figure 3.5 shows the cleaving tool. Usually the cleaving tool is designed in a way so that cleaved fiber length is about 3-5 mm. I had to do the cleaving such that it has a minimum cleaved length manually pushing the fiber toward the blade. I was skeptical about the quality of the cleaving but it came out nice. Figure 3.6 shows a smooth cleaving. To use the fiber inside the nanoscribe tool, we need to ensure a very small cleaving length. If it is not made a small cleaving length, it might break. The challenge here is to make that small cleaving length. The commercial cleaving tools cannot give the small cleaving length and so the cut for the cleaving is done manually by ensuring 250 μm coating layer is very close to the point where cleaving cut would be made. Figure 3.6 shows a sample cleaved fiber surface where 3D printing would be done.

Figure 3.5: Fiber Cleaving Tool

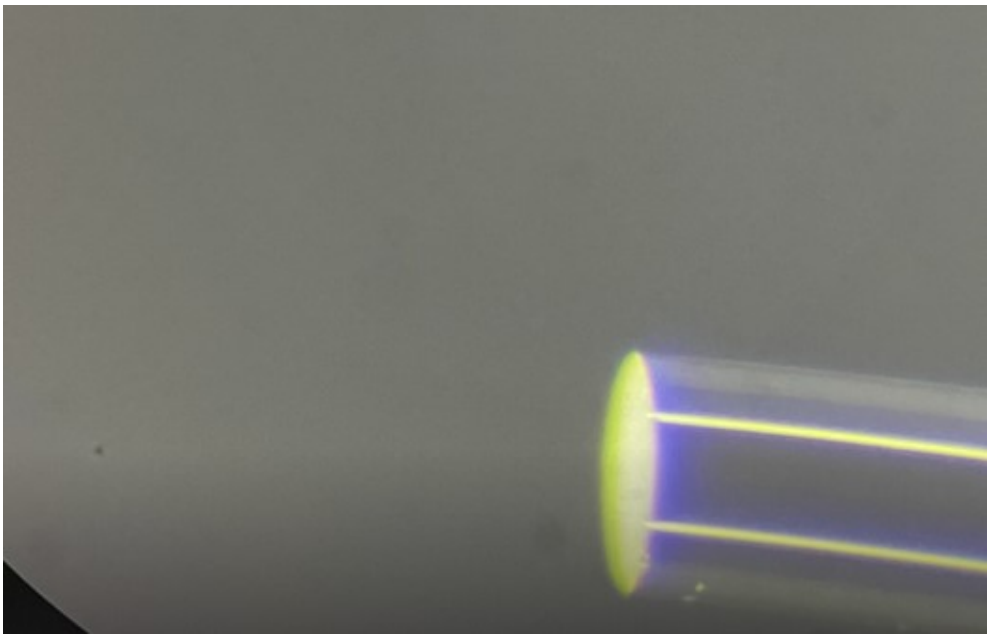

Figure 3.6: A Cleaved Fiber seen from Optical Microscope

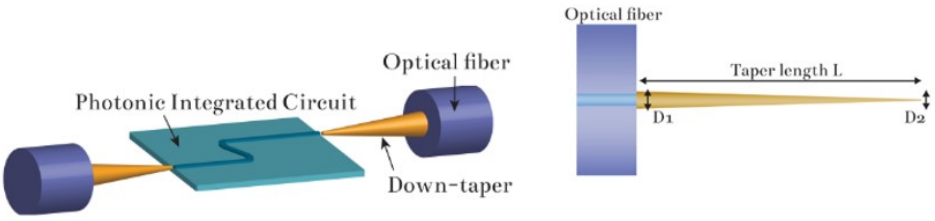

Figure 3.7: Parameters of the cones [25] [The image is taken from Vanmol et al. (2020) work to show the design parameters]

3.4 Simulation/Design at 980nm

The idea is to print cones on the cleaved fiber. The cone parameters need to be designed such that it works for a particular wavelength of light. For this design, I have focused on 980 nm wavelength. Lumerical simulation was done to verify the design. The total simulation could be split into 3 regions. First, Coupling between Fiber and adjacent diameter of the cone, second, Tapering region inside cone and third, Coupling between chip facet and cone. Before focusing on the regions, let's get familiar to the cone parameters. The cones that would be printed on cleaved fiber have the following paranmeters: D1=Diameter of the cone side that is in the fiber side, D2= Diameter of the cone side that goes near the photonic integrated circuit, L=Tapering length of the cone. Figure **??** shows the parameters.

Idea to print this on the SM fiber core comes from the fact that the design should be such that MFD of the core of the fiber matches the MFD of the larger diameter of the Polymer core (D1). Quick mode solution simulation gives the larger diameter to be around 8-9 um. Also, the smaller diameter needs to have mode matching with the facet waveguide. Assuming 150nm width taper for 440nm thick SiN waveguide, the smaller diameter of cone is 400nm, which is theoretically possible as minimum feature size of Nanoscribe tool is 200nm.

3.4.1 Coupling between fiber and the cone: designing the larger diameter D1 and optimization

To design the correct D1 parameter, the starting point was to sweep the D1 parameter and check overlap with the MFD of the SM fiber. SM 980 fiber MFD is about 5.8 micron and from Figure 3.8, it appears that 8 and 9 micron diameter value for D1 parameter works near 100% overlap. This overlap calculation was done using Lumerical Mode solution. This overlap calculation is based on the following equation:

$$overlap = Re[\frac{(\int E_1 \times \vec{H_2^*} \cdot d\vec{S})(\int E_2 \times \vec{H_1^*} \cdot d\vec{S})}{\int E_1 \times \vec{H_1^*} \cdot d\vec{S}}] \frac{1}{Re(\int \vec{E_2} \times \vec{H_2^*} \cdot d\vec{S})}$$

The two mode overlap calculation performs the fractional power coupling from profile (E2,H2) into the mode (E1,H1). The overlap does not take into account reflections due to a mismatch in effective indices between the two modes. So I chose the optimized D1=8 micron. Figure 3.9 shows the gaussian field profile for the fundamental TE mode.

3.4.2 Tapering length of Cone

Lumerical EME solver was used to find transmission vs taper length for IP-DIP(2) polymer using only linear taper. It is clear longer the taper, higher the transmission. At about 100 μm taper length we get about 80% transmission. However, longer taper seems to have issues with not sticking, bending etc. which will be discussed later.Figure 3.10 shows that as we get higher taper length, it gets toward higher transmission.

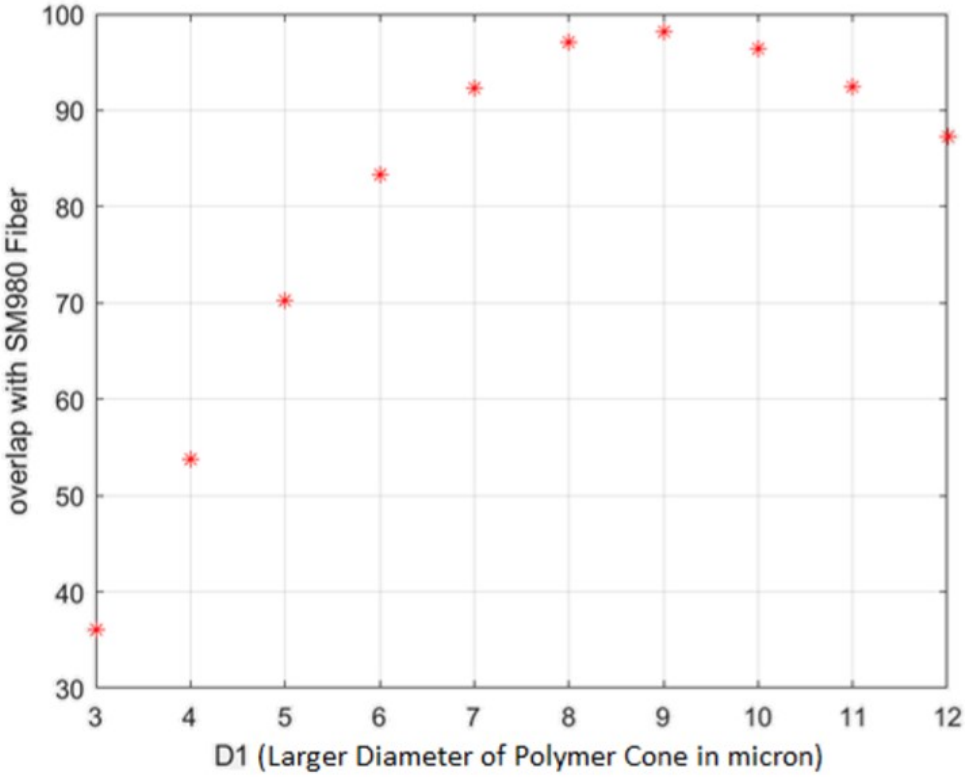

Figure 3.8: Finding the optimization from maximum overlap percentage between SM 980 fiber and printed cone

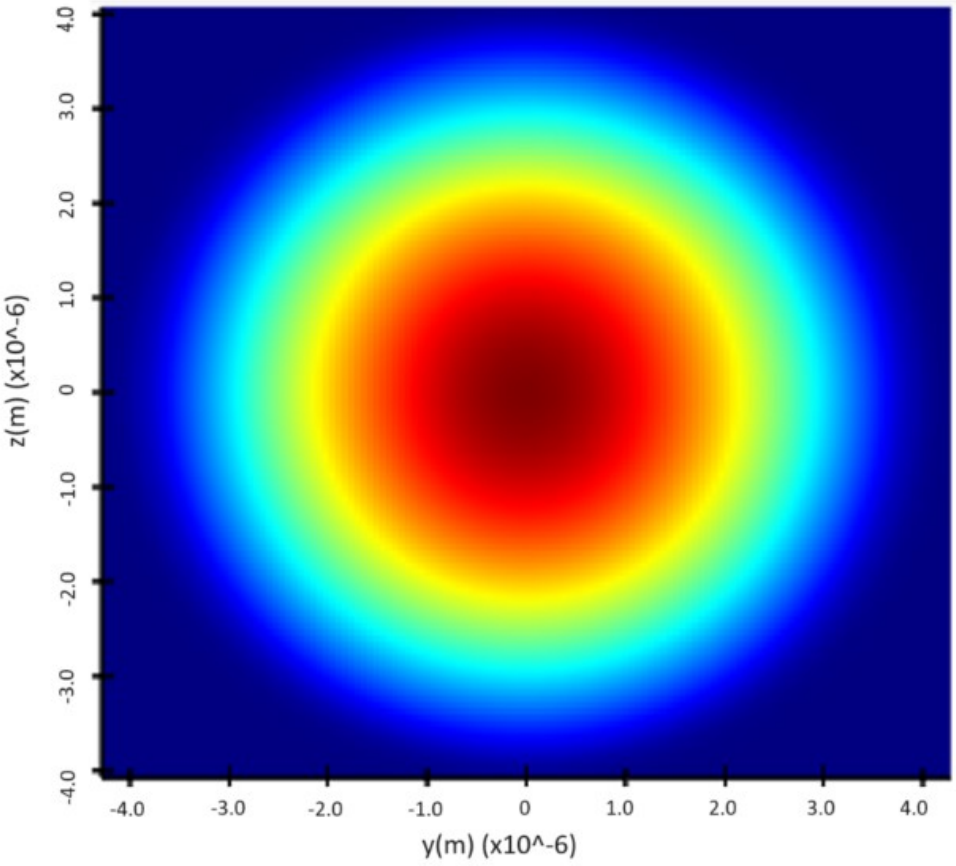

Figure 3.9: Mode profile with D1=8 micron

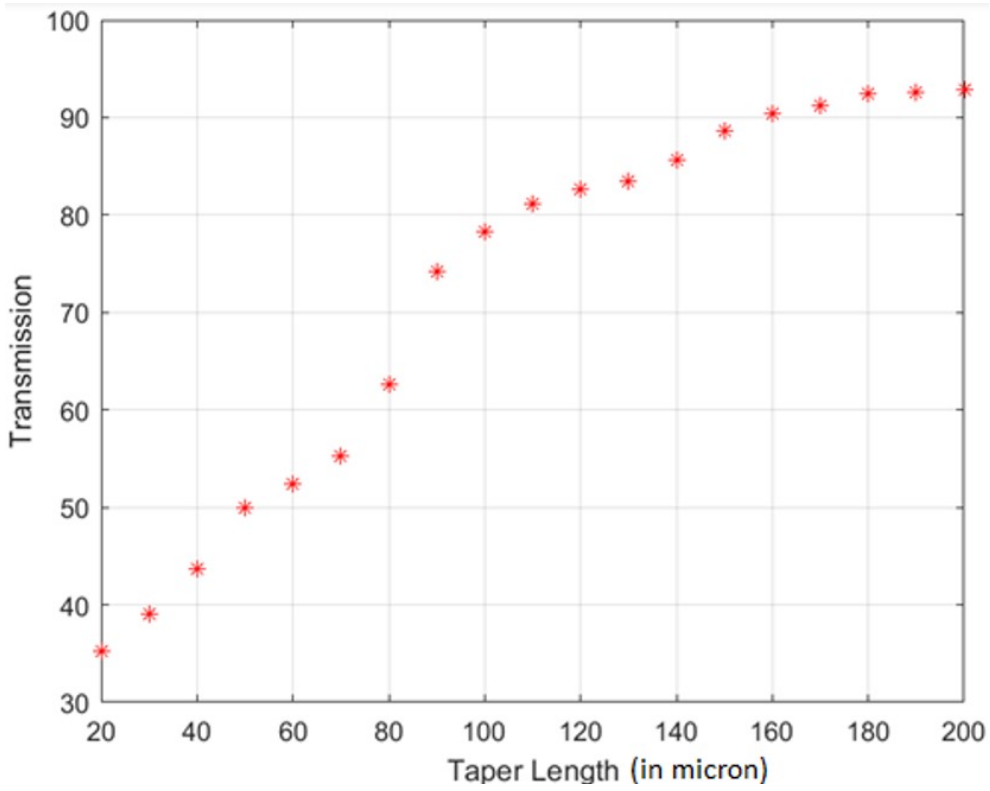

Figure 3.10: EME simulation to find the taper length

3.4.3 Coupling between chip facet and the cone: designing the smaller diameter

On the other hand, D2 denotes the smaller diameter. As it is seen from the following figure, 400 nm smaller diameter gives the best overlap. However, 2 μm also gives over 90%. In fact, 1.5-2.5 μm range could also work with over 90% overlap. Figure 3.11 shows the optimzation of D2 parameter. Figure 3.12 shows the mode profile of D2=400 nm.

3.5 CAD Design for 980 nm light

For 980 nm operation, a good design is D1=8-9 μm and D2=400nm and L=100 μm. Using solidworks, this truncated cone was generated to be used in DeScribe software of nanoscribe tool. A few other designs were tried to check the print quality. However, the nanoscribe part is

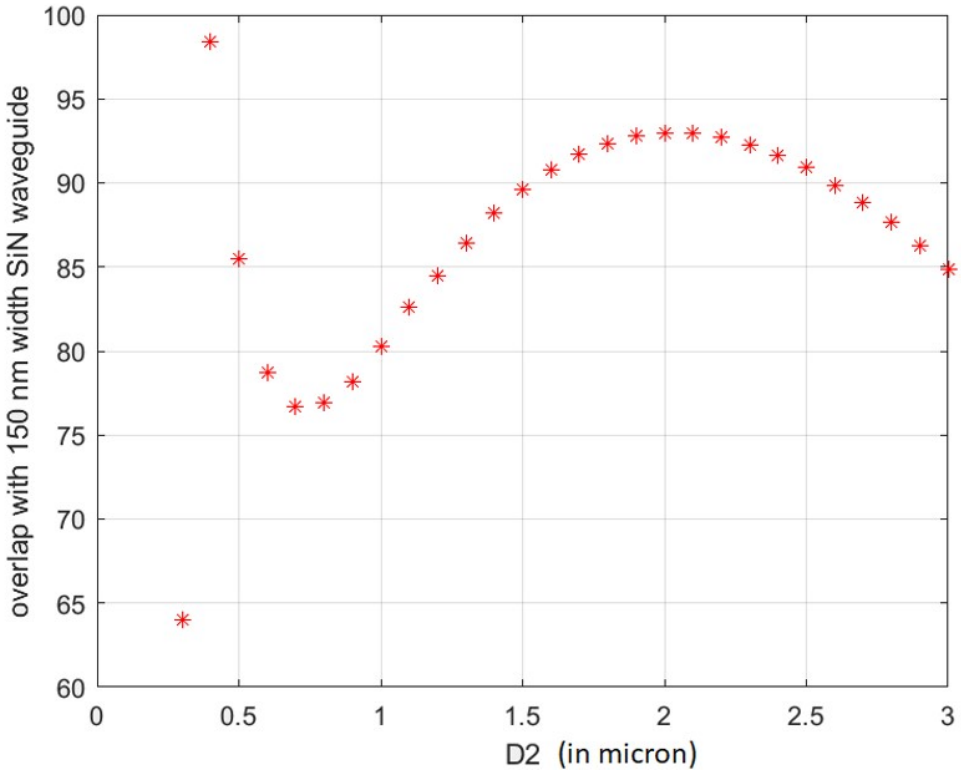

Figure 3.11: Optimizing D2

described in the next section. Figure 3.13 shows the CAD design.

3.6 Nanoscribe Fabrication

Nanoscribe fabrication was done in a few steps. I have to figure out a good way to print in the fiber core. In the meantime, the first attempt was on glass slide. A dose test was carried out to find the best dose. That dose was followed later on for the fiber.

3.6.1 Dose Testing

When we speak of dose testing, in technical terms of the nanoscribe tool a number of parameters are to be considered including Laser power, Scanspeed, slicing distance, hatching

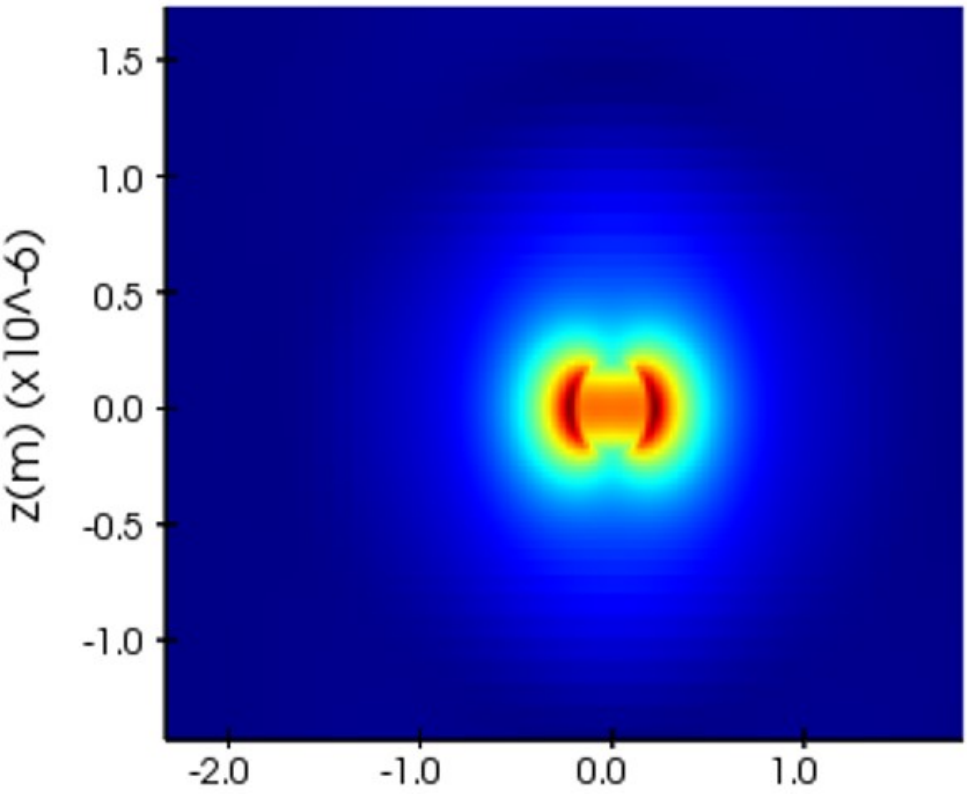

Figure 3.12: Mode Profile, D2=400nm

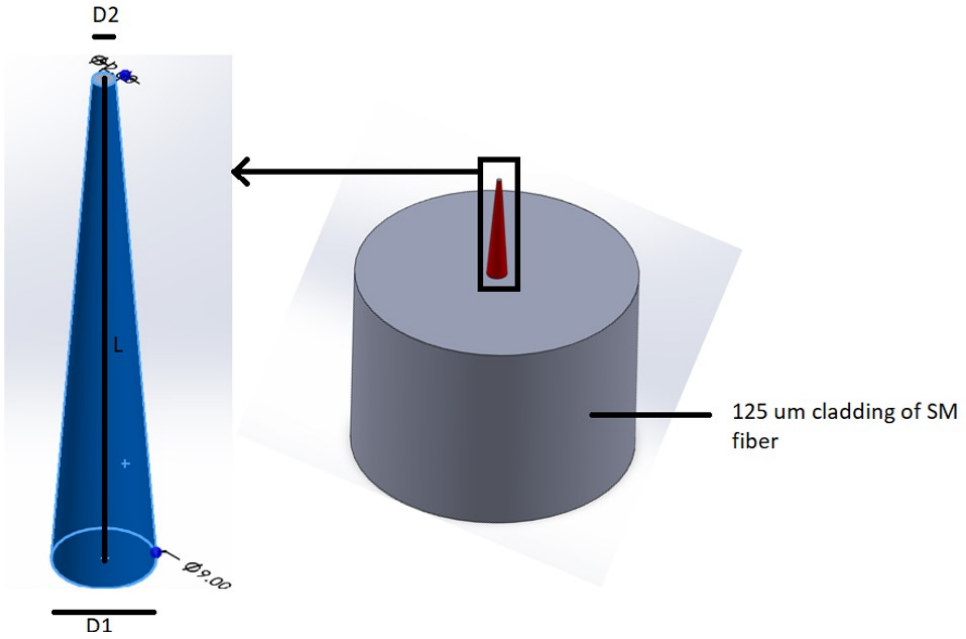

Figure 3.13: CAD design of Cone

distance, baselayers etc. But to make the dosing experiment simpler, we set the slicing and hatching distance to 100 nm and a fixed number of 50 baselayers. That leaves laser power and scanspeed as the most two important dosing parameters.

3.6.2 Fused Silica Glass Slide Print

A sweep of laser power(20 to 36%) and scan speed(5000 to 15000um/sec) was done to check the dosing impact in terms of sticking structures. Figure 3.14 shows the results. A few dosing combination would not simply stick, a few would burn and a few would stand. For IP-DIP(2) a few different combinations gave structures without washing away. A number of coarse and fine dose testing were done and the most useful ones are LP (laser power) of 30% and SS (scan speed) of 5000 um/s. Figure 3.15 shows two good prints. Some of the structures were bending (Figure 3.16) so later different taper heights were tried to check the impact of taper height. Later, some higher laser power were tried with high scanspeed which also was useful.

3.6.3 Dose testing with High Dose

The previous dose of about 30% laser power and 5000 μm/s scanspeed caused the sag for 200 μm tapers and sometimes for 100 μm taper as well, which leaves a development question that we tried to work with later. Let's see the impact of higher dose. For high dose testing, laser power 30-57% were tried with a higher scanspeed of 20000 μm/s.

To summarize, 57% laser and 20000 μm/s gives less bending for 200 μm taper. Going to higher laser power initiates burning. Figure 3.17 shows as we go to higher dose (left to right), bending issue improves.

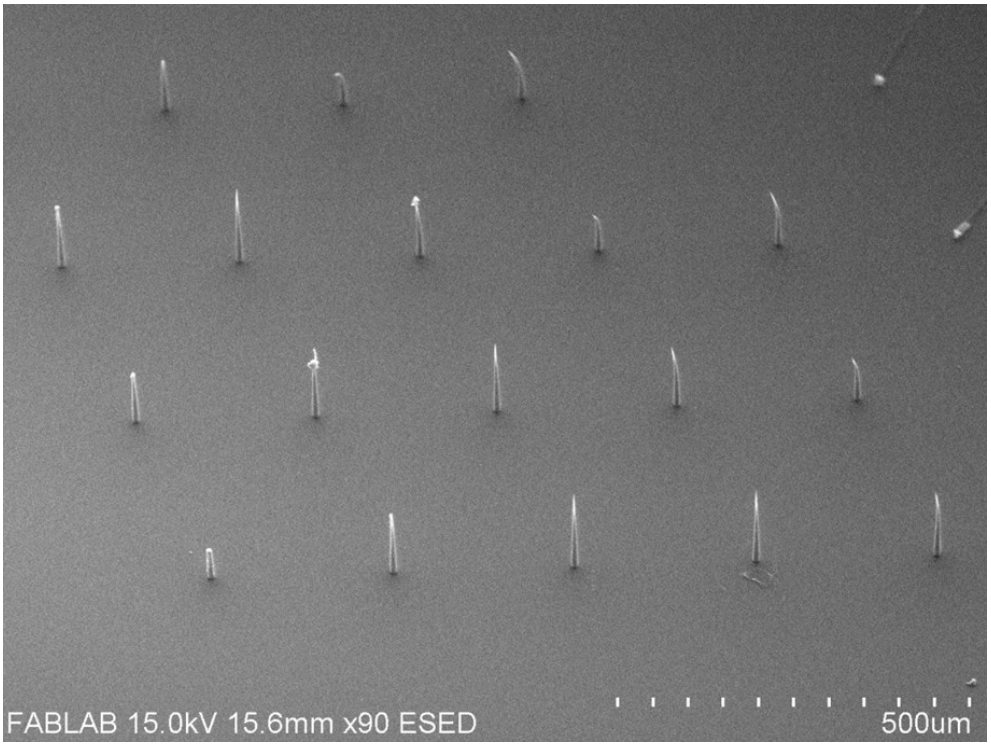

Figure 3.14: Dose Testing with IP-DIP2 resin on glass slide for 200 μm taper. Bottom row: Fixed 5000 μm/s scanspeed and varying laser power from 20-36% Second last row: Fixed 10000 μm/s scanspeed and varying laser power from 20-36% The row above: Fixed 15000 μm/s scanspeed and varying laser power from 20-36%

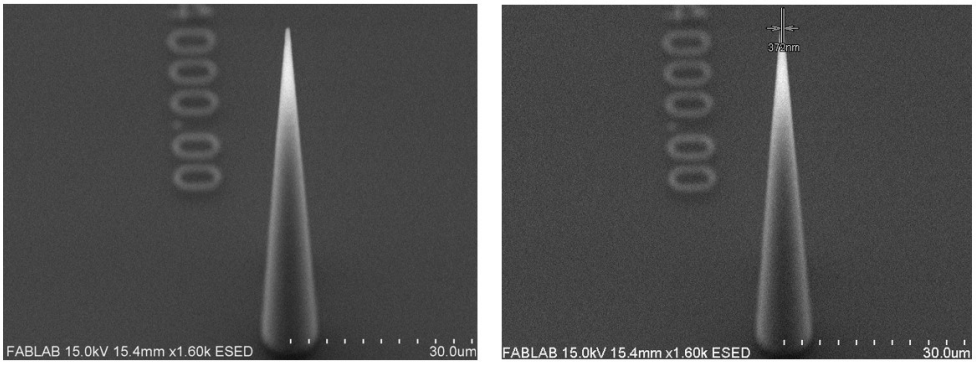

Figure 3.15: A good dose Laser Power 30% and scanspeed 5mm/s for printing 100 micron long taper

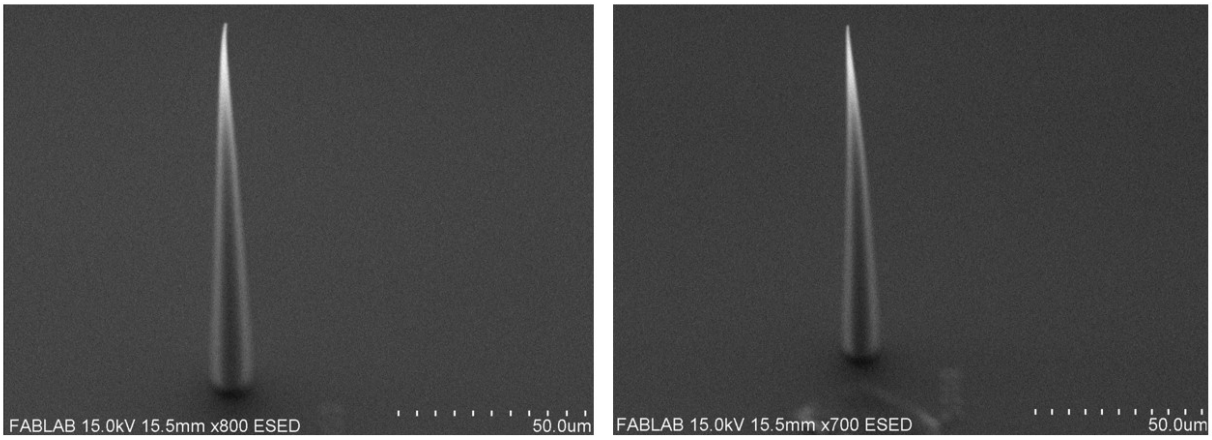

Figure 3.16: Bending scenario for a few cases (100 micron taper)

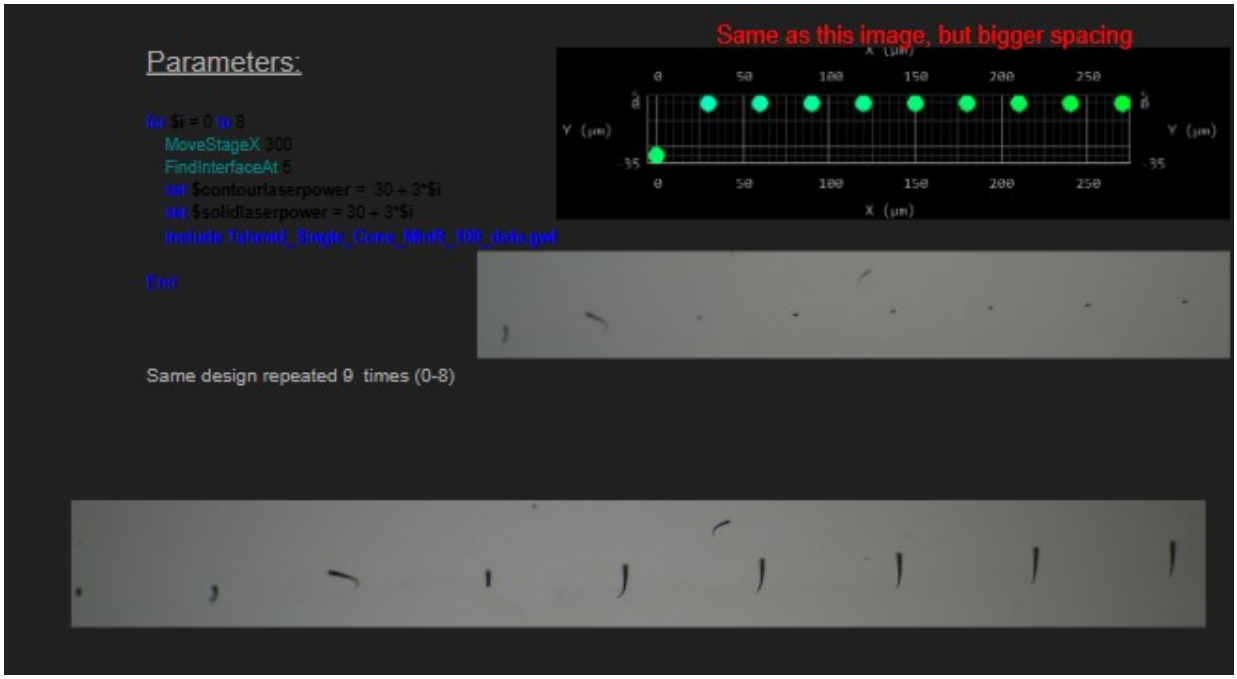

Figure 3.17: Higher laser power gives less bending (left to right)

3.7 Mounting SM fiber

Using the nanoscribe tool is straightforward, if we do it in a glass slide. But with custom printing surface, we need to be very careful so that the objective does not hit the surface or get damaged. So a few safe tries were made for placing the SM fiber inside nanoscribe tool.

3.7.1 First Trial

Nanoscribe tool has a multidill holder for placing the samples like glassslide or silicon pieces. But mounting a fiber is challenging since it is about 125 μm clad that we need to deal with. So, a manual process needs to be initiated for mounting the fiber. A blue primary holder with tapped holes were 3D printed that will hold another secondary machined mount with a central hole to hold the fiber chuck piece and other holes to be mounted to the primary holder. The secondary mount also has the set screw facility from top to make sure the fiber chuck piece is tightly attached and cannot move. The cleaved fiber is placed inside the chuck. It could hold multiple fibers at a time. Figure 3.18 shows the whole picture of the first trial of mounting SM fiber put inside a piece of chuck.

So, the silver Al metal piece (secondary holder) was machined as a 'T shape'. This process was good at the starting but gradually fiber cleaving did not seem flat in the nanoscribe microscope meaning some tilt or movement. So, a 2nd fiber mount was designed.

3.7.2 Second Trial

This secondary mount design has a longer piece with triangular looking groves to place the fiber and it also two tapped holes and two untapped holes. The untapped holes are used to mount

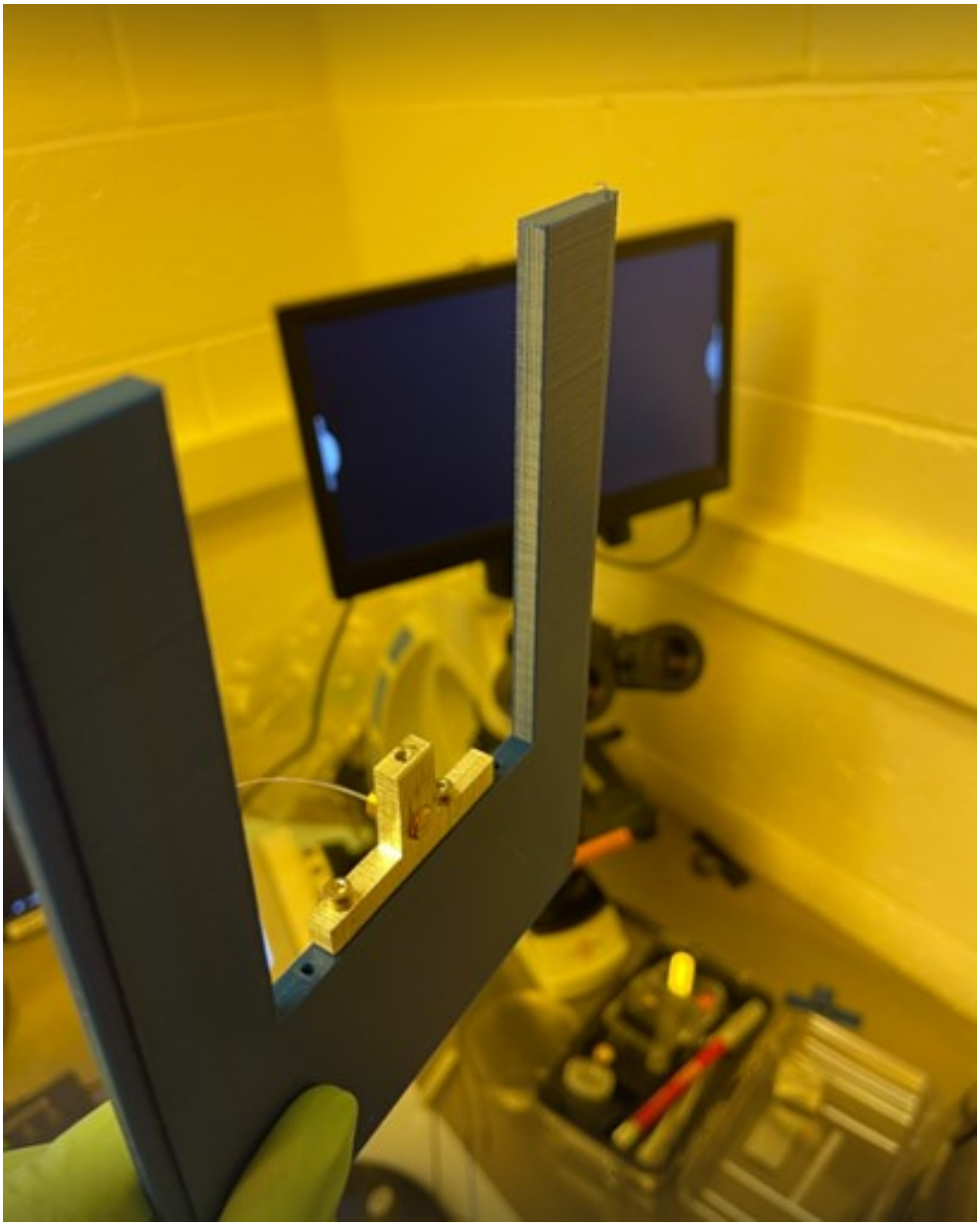

Figure 3.18: Mounting SM fiber: 1st trial- a metal piece was machined with a hole to hold a cut piece of fiber chuck and clamp it from top. This secondary piece is clamped to the primary mount (blue) before putting inside the nanoscribe tool

on the primary mount. The tapped holes are used to mount a shorter piece on top of the longer piece containing the fibers on groves. The Smaller piece sits on top this larger piece and using screws, the whole piece is tightened. Figure 3.19 shows the 2nd trial to mount the fibers without using any chuck.

We start with placing the cleaved fiber in the groove ensuring less than 300 μm is extruded outside the grove. This is due to the working distance of the objective lens. However, using the microscope, I tried to make this as minimum as possible. 300 μm is not the limit it is a bit more. But setting 300 μm as the max is safe. Figure 3.20 shows the placement of the fiber.

After the printing was done, the development was critical. It was developed upside down using PGMEA followed by IPA. Figure 3.21 shows the developed cone. Figure 3.22 shows the circular tip.

3.8 Issue with developing: Not 100% yield

The dose that worked for glass slide, unfortunately did not work every time in the fiber print. Since it is a very delicate structure, it is very sensitive during development. Some issues occurred after development. Here is a brief description for the issues:

The IP-DIP(2) photo resin based prints require a general development inside PGMEA for 15-20 mins followed by few mins rinse with IPA. In between the two steps, we also added UV bath(Intensity was 89 μW/cm^2).

6 cycles were used for 90 second/cycle to harden the polymer. UV exposure never harms but still 100% yield was never met.

However, several mishaps happened with correct dose: 1. Burn near the tip. 2. Bending at

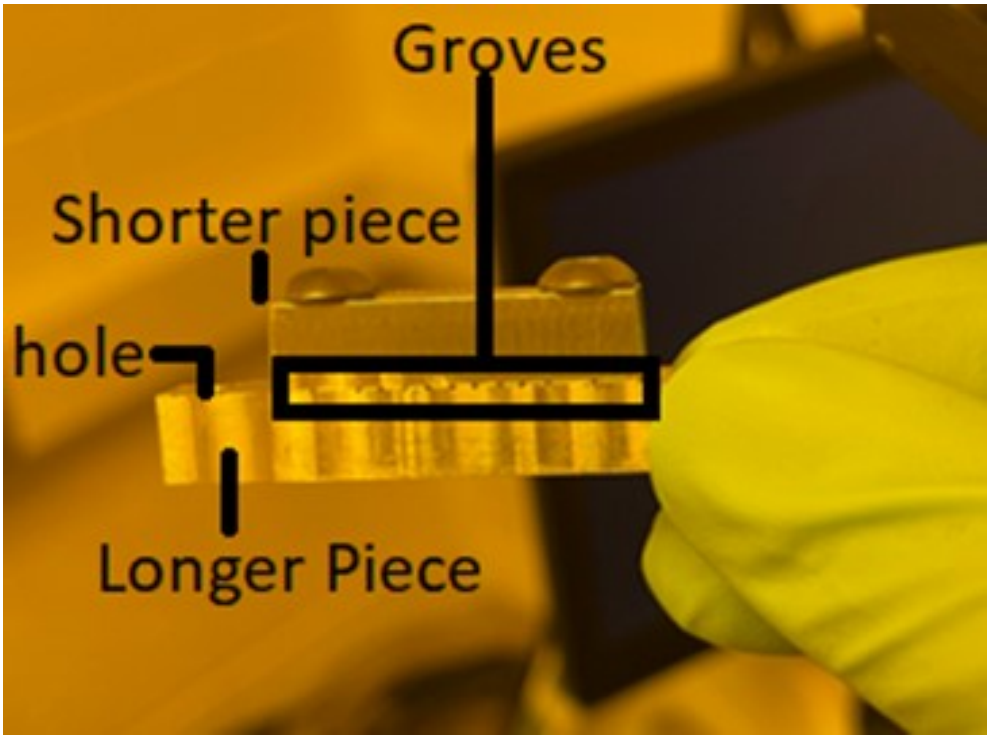

Figure 3.19: Mounting SM fiber: 2nd trial-this time fiber chuck was avoided and the clamping was ensured inside machined groves. It was carefully done so that fiber is not damaged from too tight clamping.

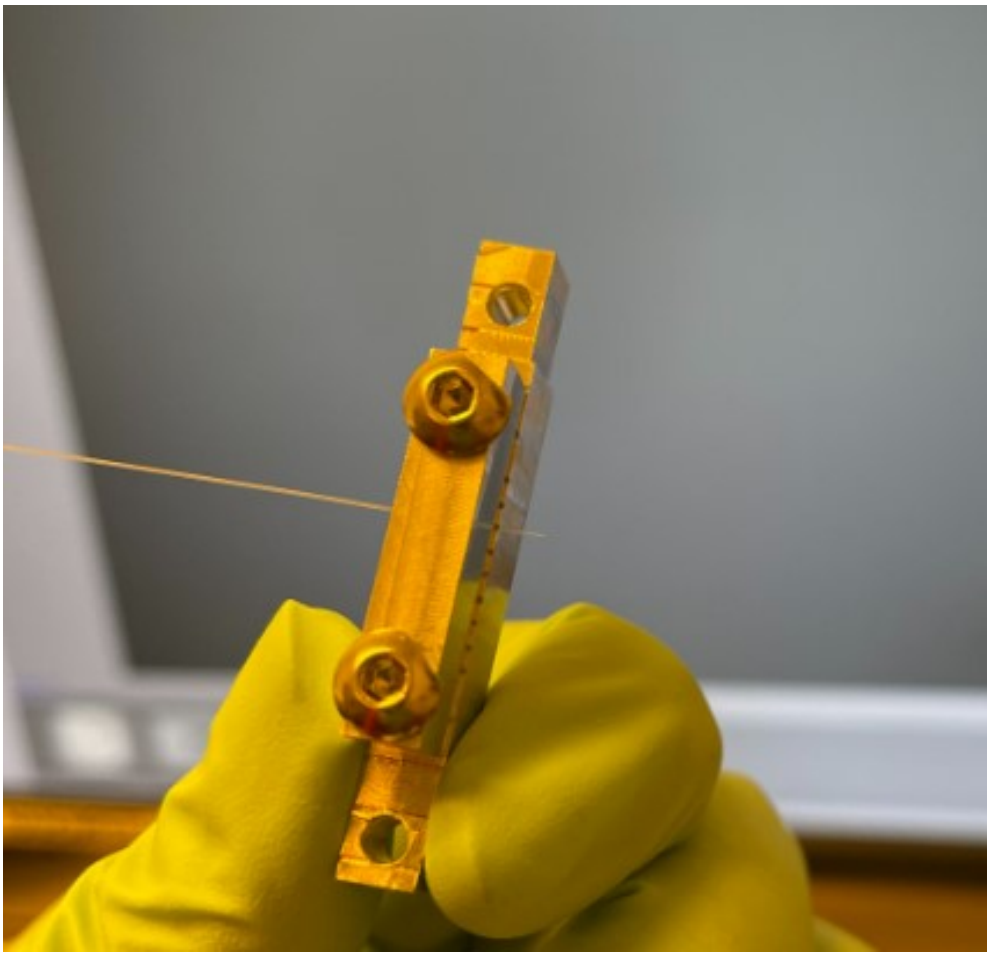

Figure 3.20: Mounting SM fiber: 2nd trial metal piece

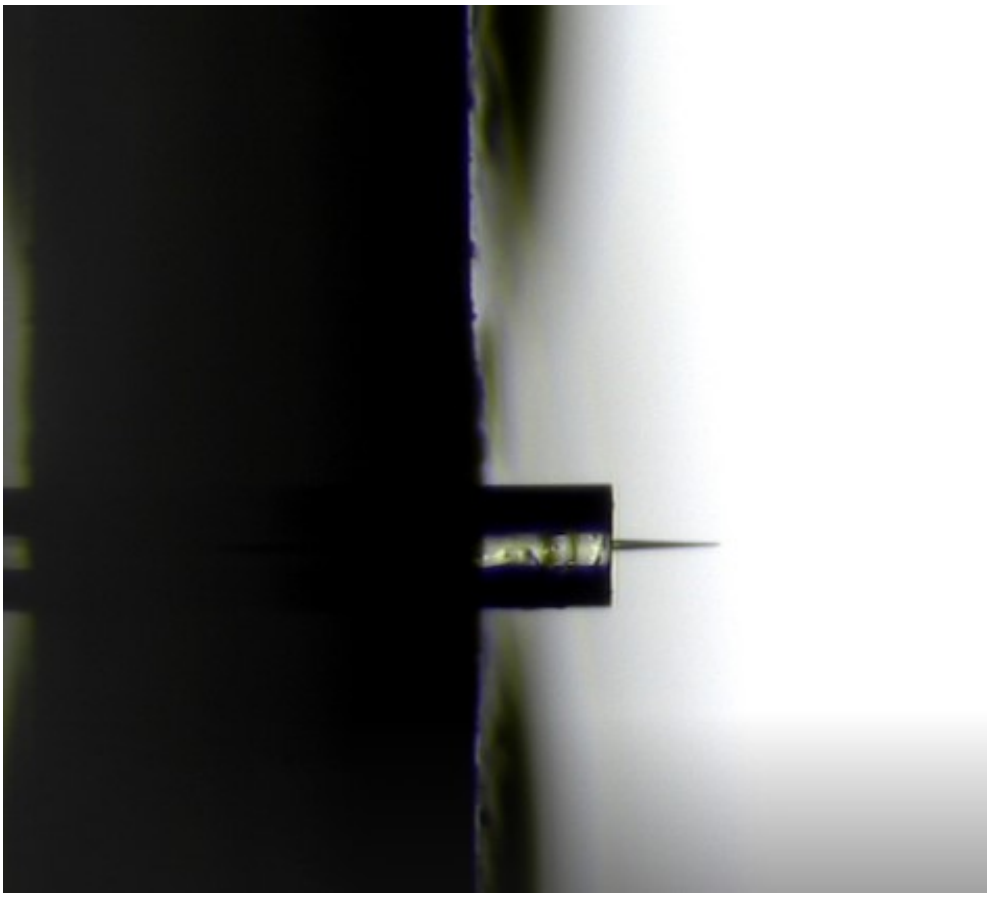

Figure 3.21: Visible Cone after development

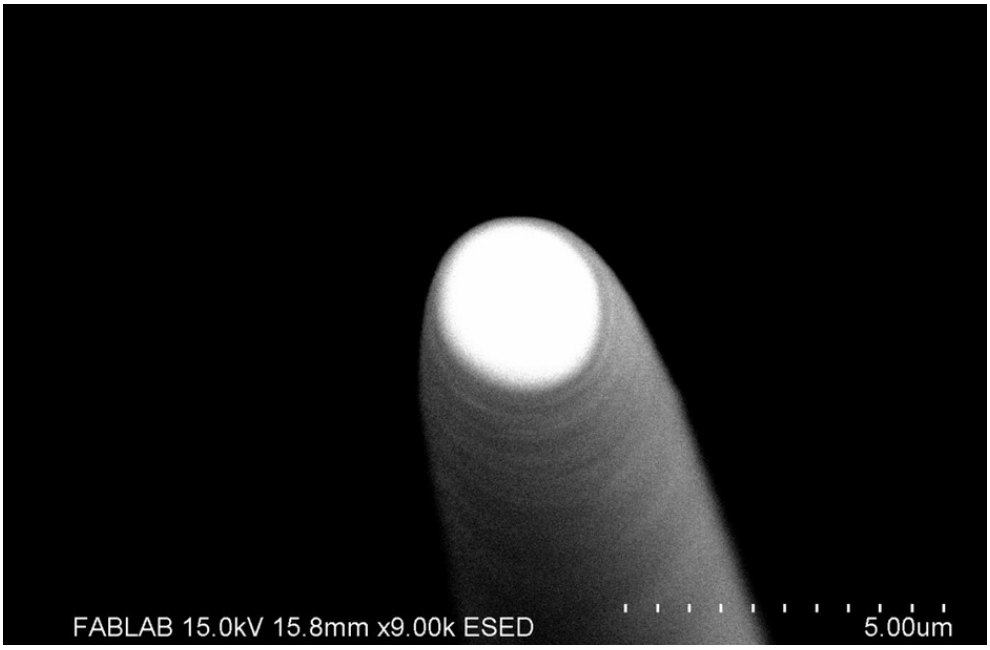

Figure 3.22: SEM tip

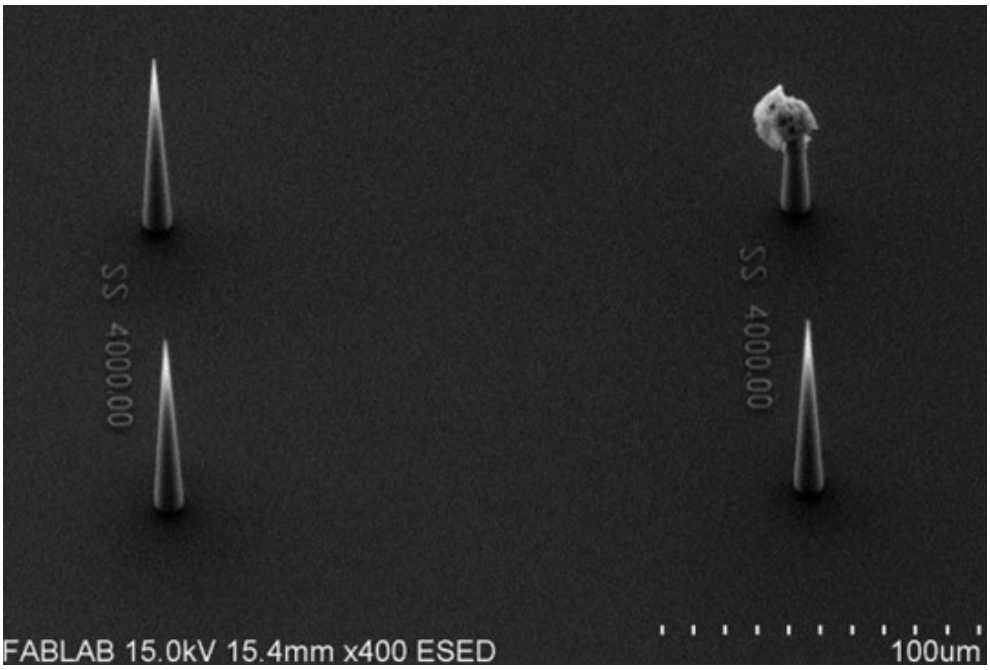

Figure 3.23: Burning occuring randomly

the designed length. 3. Burn at the fiber core interface. 4. Fallen structures.

3.8.1 Burn near the tip:

Sometimes burn near the tip was observed which was visible clearly in the nanoscribe microscope just before the end of the print. The problem was solved with increasing the slicing distance. The possible explanation is that when the tip is about 300 nm but the voxel size is about 250 nm, voxels might overlap and cause heating and burning at the very tip with the neighbor slices. Figure 3.23 shows a clar burning case during printing in fused silica.

3.8.2 Bending Issue

Printing the design often ends without any hassle but the development of these couplers is quite sensitive. There are three possible development style. The main development is with

Figure 3.24: Bending of cones

PGMEA as mentioned before but that development could be done rightside up or upside down or from the side. All three types were tried, but the bending phenomenon was always present. Figure 3.24 shows a slight bend after development. Alternate development could be tried with NOVEC 7100 instead of PGMEA.

3.8.3 Burning near fiber core

Sometimes at the beginning of the print a clear bubble occurs due to dose not matched well. Figure 3.25 shows this type of burning. So, the best dose was chosen from glass slide testing and the same dose is applied on the fiber print. But there could be anchoring issues for fiber case causing additional heat as we start the print a little bit (5-10 μm) inside to ensure adhesion. For

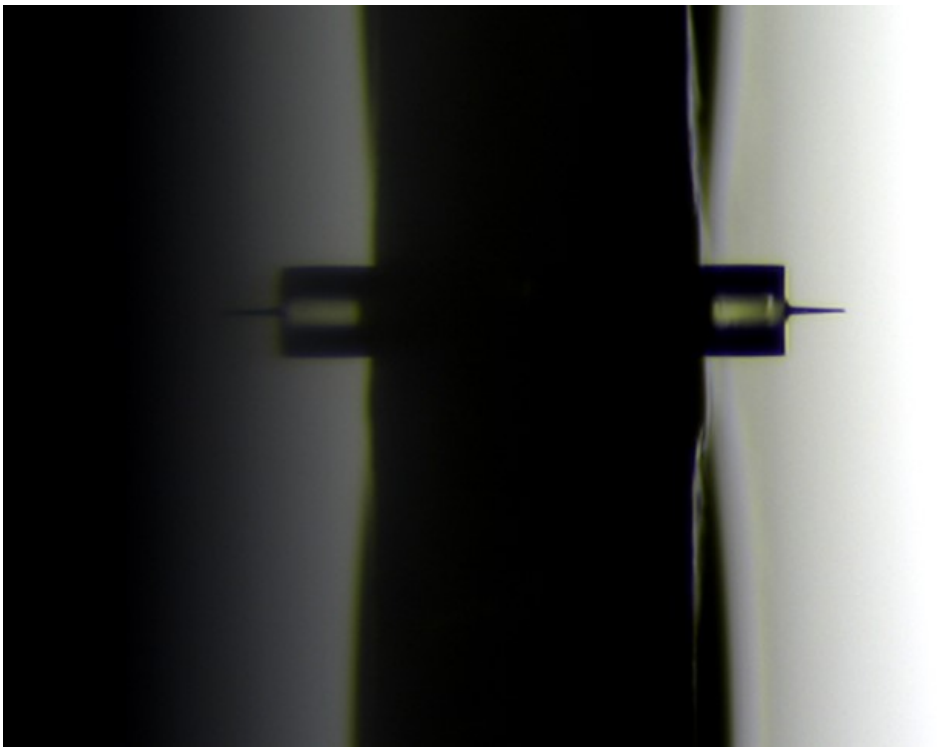

Figure 3.25: Burning near the fiber core at the start of printing

glass, autofocus could find the interface and the print started based on that. But for fibers, it needs a manual touch. Also surface area for glass slide is larger than fiber so the heat or burn might occur sometimes.

3.8.4 Fallen Structure

Usually mismatch of dose causes structures to wash away. But we have occasionally found the fallen structure with allowed dose as well. There could be some relation between aging of photoresins and dose as well.

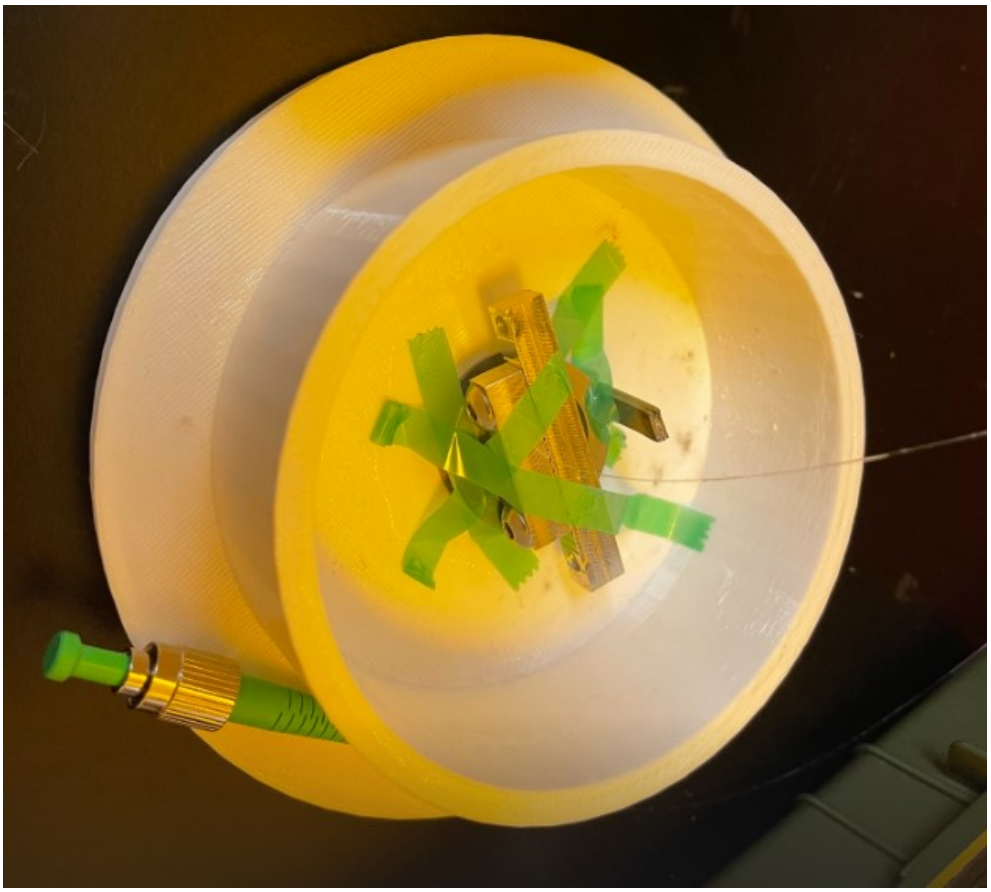

Figure 3.26: Upsidedown placement of the fiber in the secondary mount before submerging into PGMEA

3.9 Development of the Delicate Cones

Development of the cones are very sensitive. They might be affected by bubble from the development chemical. So, rightside up method was not attempted much as most of the time it failed. It is obvious that the structure would face maximum force in this process. I tried side development and upside down development. Upside down development gave the maximum yielding (figure 3.26). It is easier to develop fibers upside down and using our secondary mount it is ensured that the fiber remains upside down. Taping the mount, we use PGMEA for 15-20 mins for the main development followed by UV and rinsing with IPA.

3.10 Experimental Approach

Only when taper lengths are 50 μm, the yield is about 100% and two devices were tested for insertion loss. The results were not very great as optimized taper length without bending was not met and there are no automatizing of aligning the print with the core of fiber. Lensed fiber-Lensed fiber combination was giving 2.7 dB loss while Lensed fiber-cone on SM fiber was giving about 4.8 dB loss. So the upcoming challenge is to ensure that development process do not affect the structure and the loss should be improved.

Bibliography

[1] T Alder, A Stohr, R Heinzelmann, and D Jager. High-efficiency fiber-to-chip coupling using low-loss tapered single-mode fiber. *IEEE Photonics Technology Letters*, 12(8):1016–1018, 2000.

[2] Nadya Anscombe. Direct laser writing. *Nature Photonics*, 4(1):22–23, 2010.

[3] Krishna C Balram, Daron A Westly, Marcelo Davanco, Karen E Grutter, Qing Li, Thomas Michels, Christopher H Ray, Liya Yu, Richard J Kasica, Christopher B Wallin, et al. The nanolithography toolbox. *Journal of Research of the National Institute of Standards and Technology*, 121:464, 2016.

[4] Andrea Bertoncini and Carlo Liberale. Polarization micro-optics: circular polarization from a fresnel rhomb 3d printed on an optical fiber. *IEEE Photonics Technology Letters*, 30(21):1882–1885, 2018.

[5] LP Boivin. Thin-film laser-to-fiber coupler. *Applied Optics*, 13(2):391–395, 1974.

[6] CH Bulmer, SK Sheem, RP Moeller, and WK Burns. High-efficiency flip-chip coupling between single-mode fibers and linbo3 channel waveguides. *Applied Physics Letters*, 37(4):351–353, 1980.

[7] Lifeng Chen, Haozhi Luo, and Xinlun Cai. 3d micro lenses for efficient edge coupling by two-photon lithography. In *2021 Conference on Lasers and Electro-Optics (CLEO)*, pages 1–2. IEEE, 2021.

[8] P-I Dietrich, M Blaicher, I Reuter, M Billah, T Hoose, A Hofmann, C Caer, Roger Dangel, B Offrein, U Troppenz, et al. In situ 3d nanoprinting of free-form coupling elements for hybrid photonic integration. *Nature Photonics*, 12(4):241–247, 2018.

[9] H Gehring, M Blaicher, W Hartmann, P Varytis, K Busch, M Wegener, and WHP Pernice. Low-loss fiber-to-chip couplers with ultrawide optical bandwidth. *APL Photonics*, 4(1), 2019.

[10] Helge Gehring, Alexander Eich, Carsten Schuck, and Wolfram HP Pernice. Broadband out-of-plane coupling at visible wavelengths. *Optics letters*, 44(20):5089–5092, 2019.

[11] Wisnu Hadibrata, Heming Wei, Sridhar Krishnaswamy, and Koray Aydin. Inverse design and 3d printing of a metalens on an optical fiber tip for direct laser lithography. *Nano letters*, 21(6):2422–2428, 2021.

[12] HP Hsu and AF Milton. Flip-chip approach to endfire coupling between single-mode optical fibres and channel waveguides. *Electronics Letters*, 16(12):404–405, 1976.

[13] Robert G Hunsperger, A Yariv, and A Lee. Parallel end-butt coupling for optical integrated circuits. *Applied optics*, 16(4):1026–1032, 1977.

[14] Kazuo Kasaya, Osamu Mitomi, Mitsuru Naganuma, Yasuhiro Kondo, and Yoshio Noguchi. A simple laterally tapered waveguide for low-loss coupling to single-mode fibers. *IEEE photonics technology letters*, 5(3):345–347, 1993.

[15] Hideo Kuwahara, M Sasaki, and N Tokoyo. Efficient coupling from semiconductor lasers into single-mode fibers with tapered hemispherical ends. *Applied Optics*, 19(15):2578–2583, 1980.

[16] IF Lealman, LJ Rivers, MJ Harlow, and SD Perrin. Ingaasp/inp tapered active layer multiquantum well laser with 1.8 db coupling loss to cleaved singlemode fibre. *Electronics Letters*, 30(20):1685–1687, 1994.

[17] Fabian Niesler and Martin Hermatschweiler. Two-photon polymerization—a versatile microfabrication tool: From maskless lithography to 3d printing. *Laser Technik Journal*, 12(3):44–47, 2015.

[18] Juichi Noda, Osamu Mikami, Makoto Minakata, and Masaharu Fukuma. Single-mode optical-waveguide fiber coupler. *Applied optics*, 17(13):2092–2096, 1978.

[19] Nair S Parvathi, Jonathan Trisno, Hongtao Wang, and Joel KW Yang. 3d printed fiber sockets for plug and play micro-optics. *International Journal of Extreme Manufacturing*, 3(1), 2021.

[20] Maura Power, Alex J Thompson, Salzitsa Anastasova, and Guang-Zhong Yang. A monolithic force-sensitive 3d microgripper fabricated on the tip of an optical fiber using 2-photon polymerization. *Small*, 14(16):1703964, 2018.

[21] Mariacristina Rumi and Joseph W Perry. Two-photon absorption: an overview of measurements and principles. *Advances in Optics and Photonics*, 2(4):451–518, 2010.

[22] RV Schmidt and LL Buhl. Experimental 4 x 4 optical switching network. *Electronics Letters*, 12:575–577, 1976.

[23] Martin Schumann, Tiemo Bückmann, Nico Gruhler, Martin Wegener, and Wolfram Pernice. Hybrid 2d–3d optical devices for integrated optics by direct laser writing. *Light: Science & Applications*, 3(6):e175–e175, 2014.

[24] Gyeongho Son, Seungjun Han, Jongwoo Park, Kyungmok Kwon, and Kyoungsik Yu. High-efficiency broadband light coupling between optical fibers and photonic integrated circuits. *Nanophotonics*, 7(12):1845–1864, 2018.

[25] Koen Vanmol, Kumar Saurav, Vivek Panapakkam, Hugo Thienpont, Nathalie Vermeulen, Jan Watté, and Jürgen Van Erps. Mode-field matching down-tapers on single-mode optical fibers for edge coupling towards generic photonic integrated circuit platforms. *Journal of Lightwave Technology*, 38(17):4834–4842, 2020.

[26] Koen Vanmol, Salvatore Tuccio, Vivek Panapakkam, Hugo Thienpont, Jan Watté, and Jürgen Van Erps. Two-photon direct laser writing of beam expansion tapers on single-mode optical fibers. *Optics & Laser Technology*, 112:292–298, 2019.

[27] Heming Wei, Maoqing Chen, and Sridhar Krishnaswamy. Three-dimensional-printed fabry–perot interferometer on an optical fiber tip for a gas pressure sensor. *Applied optics*, 59(7):2173–2178, 2020.

[28] Amnon Yariv and Pochi Yeh. *Photonics: optical electronics in modern communications*. Oxford university press, 2007.